An integrated planning model in centralized power systems

Francisco López-Ramos, Stefano Nasini, Mohamed H. Sayed

Version of Record: https://www.sciencedirect.com/science/article/pii/S0377221720304173
Manuscript_25453338afde3b0dd8d317c0d2bbe5fc

An integrated planning model in centralized power systems

Francisco López-Ramos[a], Stefano Nasini[b,c,*], Mohamed H. Sayed[d]

[a]*Innovation Laboratory of Applied Electronics, National Council for Science and Technology, México*
[b]*IESEG School of Management, 3 rue de la Digue, 59000 Lille, France.*
[c]*LEM-CNRS 9221, 3 rue de la Digue, 59000 Lille, France.*
[d]*Sale Management, Schneider Electric SE, France.*

Abstract

In the context of centralized electricity markets, we propose an integrated planning model for power pricing and network expansion, which endogenizes the scaling costs from power losses. While the substitutability pattern between pricing and expansion has been overlooked in the power flow optimization literature, this becomes particularly relevant in centralized electricity markets (where the headquarters are enabled to take decisions over a wide range of operational factors). In this paper, we tailor an optimization model and solution approach, that can be effectively applied to large-scale instances of centralized power systems. Specifically, we develop bounds to the optimal operator profit and use them within a mixed-integer linear programming problem, derived from the linearization of an extended power flow model. On the empirical side, we conduct computational tests on a comprehensive power system data set from the Saudi Electricity Company, uncovering the value of the proposed integrated planning. The results reveal the complex substitutability patterns which appear when deciding about integrated operational factors in centralized power systems and support the correctness and efficiency of the proposed resolution mechanism.

Keywords: OR in Energy; Centralized electricity markets; Integrated pricing and expansion; Power network flow; Linearization-approximation

1 Introduction

In the context of centralized electricity markets, a single company is in charge of the electricity production at generation facilities, as well as its distribution to the end consumers throughout a power network. Despite the alternatives to replace this paradigm with decentralized grids (Roh et al. 2007, Le Cadre et al. 2015), centralized systems are still attractive for the large economy of scale and positive spillovers they rely upon.

One important benefit of centralized electricity markets is that these systems enable simultaneous decisions on electricity pricing and network expansion, driving a profitable integrated policy from their effects on power demand and distribution costs.[1] In fact, while prices have a direct impact on the total company revenue, they affect indirectly the scaling distribution costs, through their relations with power demands. This indirect effect acts on the company cost structure by causing variations on the power flow at each transmission line, similar to the outcome of building (or dismantling) parallel lines.

How this substitutability pattern between pricing and expansion translates into profit depends on the specific scaling behaviour of electricity distribution costs from large generation facilities to the end consumers. In fact,

*Corresponding author
Email addresses: francesc.lopezr@gmail.com (Francisco López-Ramos), s.nasini@ieseg.fr (Stefano Nasini), mohamed.hosny@outlook.de (Mohamed H. Sayed)

[1]Throughout this work, the term *policy* is employed to refer to an integrated strategy used by a centralized agency to regulate the electricity market in a unified way.

these scaling costs are driven by the presence of power losses at transmission level across the interconnected sub-networks, inducing a congestion-like type of cost on the electricity company.[2]

While the integrated pricing and expansion planning can counterbalance the impact of these scaling costs, the resulting decisional trade-off gives rise to a complex combinatorial problem, whose dependency structure has been largely overlooked in the recent literature. One reason for this neglect can be attributed to the growing emphasis given to decentralized electricity markets (Le Cadre et al. 2015, Lohmann & Rebennack 2016, Al-Gwaiz et al. 2016, Steeger & Rebennack 2017, Aussel et al. 2019), in which electricity prices and investment decisions are taken by different agents. Another reason is the increase in the model size as well as the appearance of different sources of non-linearities in the resulting formulations, which make its solvability more challenging for state-of-the-art optimization solvers.

This work proposes an Extended DC Power Flow model (EDCPF from now on) derived from the linearization of an original AC model, for the analysis of the integration and substitution between pricing and expansion in the context of a centralized electricity market. This model relies on a multi-partite network in which the power flow originates at generation stations, passes through transmission substations and terminates at consumption centers (cities and towns). In this model, a profit maximizer electricity company selects the optimal combination of price levels (affecting the total flow through demand sensitivity), capacity expansion (affecting the total flow through impedance reduction), generation and recovery (counterbalancing power losses). Because of the stochasticity of power demands, the proposed EDCPF model is embedded within a two-stage stochastic program, where losses (and recovery from dedicated equipments) are formulated as distinct flows interacting at substations.

For the computational resolution, we rely upon different levels of reformulation, approximating the original model by a mixed-integer linear program (MILP from now on), which is then solved in a four-step procedure. First, an upper bound (UB from now on) is obtained by removing power losses from the MILP. Second, using the obtained power flow as an initial solution, we define interpolation knots for a piecewise linear approximation of the power losses curve. Third, we solve a linear program representing a lower bound (LB from now on) to the optimal profit by using the so defined piecewise approximation and fixing all integer variables to the previously obtained optimal values. Fourth, we solve the complete MILP problem by requiring the profit to be within LB and UB, while using the interpolation knots given at the second step.

This four-step procedure resulted particularly effective in practice, as revealed by comprehensive computational tests conducted on a large-scale power system from the Southern Region of Saudi Arabia. Specifically, the proposed empirical assessment relies on detailed data from the Saudi Electricity Company (SEC from now on). The Southern Region network (managed by an independent authority within SEC) contains 383 stations and 402 transmission lines, distributing power toward 163 consumption centers. The station capacities are only working at their 46 % on average, and the network connectivity is significantly low (only 1.2 % of the possible feasible lines are constructed).

Focusing on the simultaneous decision on pricing and expansion (while endogenizing the impact of power losses and recovery), we show that when the construction costs increase, the network expansion effect on profit can be substituted by a combination of pricing and recovery adjustment to correct marginal excess of consumption and losses that can be hardly compensated. Building on a factorial computational experiment, we explore the differences in the optimal expansion when prices are fixed and when prices are jointly decided. Similarly, to assess the impact of the aforementioned scaling costs, the same tests are performed under the cases

[2]While modern advances on material engineering (Rajarman et al. 1998) have boosted important enhancements on lessening line impedance, its scaling effect on large power systems has still foremost consequences on transmission losses (Jenabi et al. 2015, Papier 2016, Shen et al. 2018, Kovacevic 2019). Often, losses are compensated by dedicated recovery equipments (such as synchronous condenser), which act locally at substations.

when looses are not considered and when losses are not recovered. The results reveal substantial expansion variations, induced by the lack of integration, as well as an underestimation/overestimation of the expected profit. Overall, the proposed methodology allows SEC to assess the opportunity to increase the station capacities and the number of transmission lines, when alternative decisions on pricing can act as operational substitutes. At the same time, we show that this significant improvement on the company' expected profit is achievable with a low computational times within the solution approach.

The rest of the paper is organized as follows. In Section 2, we survey the relevant studies on the optimal power flow problem highlighting the contributions of the proposed approach. In Section 3, we identify the ecosystem related to the problem formulation and set up the EDCPF model. In Section 4, we provide an analytical assessment of the policy integration and substitution in the proposed EDCPF model. In Section 5, we describe the solving approach. In Section 6, we present the real network data obtained in cooperation with SEC. A large collection of computational experiments on SEC data set are being analyzed in Section 7. Finally, Section 8 concludes the paper with directions for further research. Supplementary material and mathematical proofs have been reported in Appendix A.

2 Literature review

This work is connected to several streams of literature, pivoting around the purported optimal power flow problem and its extensions to electricity pricing and capacity expansion (Frank et al. 2012a,b, Frank & Rebennack 2016, Krasko & Rebennack 2017). Hereafter, they are grouped into four domains in which we highlight the relationship with our contribution.

Optimal power flow problem. Dommel & Tinney (1968) present the first mathematical programming formulation of the optimal power flow problem with control variables, followed by contributions focusing on several specific variants (Garver 1970, Carpentier 1979). Decades later, Romero et al. (2002) propose the first extension to case of transmission expansion, comparing four formulations: a DC power flow model, a transportation model, a hybrid model, and a disjunctive model. Contextually, our approach integrates the constraints traditionally present in state-of-the-art AC models and provides a mathematical programming treatable reformulation.

Power generation. A growing number of operations research contributions have covered the production side of the electricity market (Lahdelma & Hakonen 2003, Al-Gwaiz et al. 2016, Fischetti & Pisinger 2018, Lara et al. 2018). Building on the optimal power flow framework of Romero et al. (2002), Olave-Rojas et al. (2017) incorporate the energy storage systems into the power generation, followed by a recent extension to the case of wind-based electricity generation by Zhou et al. (2019). As our model has been tailored for annual level data, power storage is not taken into account, avoiding the analysis of daily fluctuations, having marginal impact on the long run pricing and expansion policy. Additionally, the different energy sources are considered in aggregate production, as fossil-based energy sources account of 98 % of the generated power in SEC.

Power distribution and network design. When looking at the power distribution, traditional models largely formulate the power system as a bi-partite network, where generators are located in one layer, while consumption centers are in the other. The first attempt to tackle general network topologies is the work of Jensen & Bhaumik (1977), where the efficient solution of a generalized-flow problem capturing losses in water resources and electrical networks is addressed. Subsequent works overlooked the impact of network topological properties on power losses, mainly focusing on resilience to failures and robustness to exogenous shocks (Benavides et al. 2013, Wang et al. 2016). Our approach addresses the issue of the energy distribution topology from the outlook of multi-partite power networks, where multiple layers of intermediary substations mediate the transmission

from generators to consumption centers. We study the creation of new lines between disconnected substations and their enlargement to mitigate the scaling costs induced from power losses.

Power demand. Traditional models have considered power demand as an exogenous term, which is either deterministically (Benavides et al. 2013, Correa-Florez et al. 2014, Jenabi et al. 2015, Wang et al. 2016, Lara et al. 2018) or stochastically (Waller & Ziliaskopoulos 2001, Atamtürk & Zhang 2007, Lium et al. 2009) specified. In this vein, Shen et al. (2018) propose an alternative probabilistic approach to deal with exogenous stochastic demands, based on interval uncertainties on power flow, and Zou et al. (2019) study a multi-stage stochastic version of Lara et al. (2018) model. Conversely, endogenous demand models have been mainly considered in the context of decentralized electricity markets, where consumers can switch between competing operators (Roh et al. 2007, Özdemir et al. 2016). Unlike the bulk of contributions, our model considers a stochastic demand whose distribution is sensitive to prices.

Power pricing. Power pricing has been studied in the context of endogenous demand models (Le Cadre et al. 2015, Lohmann & Rebennack 2016, Steeger & Rebennack 2017, Aussel et al. 2019). Some economic oriented contributions have focus on pricing from the viewpoint of the social welfare (Lohmann & Rebennack 2016) or the producer profit (Kovacevic 2019) maximization. Kök et al. (2016) study the impact of power prices on the renewable energy investments and carbon emissions. Most formulations rely on leader-follower games that bring non-convexity and entails substantial computational challenges. Our model considers a collection of price variations (with arbitrary levels of granularity) from the current prices at each consumption center, allowing for a discrete reformulation of the power demand.

3 Problem formulation and modeling

This section proposes a static (one-shot) stochastic problem for integrated decisions on prices and expansion in centralized power systems, that endogenizes the scaling cost from power losses.[3]

3.1 Baseline definitions and notation

We start by considering a power system composed by multiple layers. Following Ahuja et al. (1993), a graph $\mathcal{G} = \langle \mathcal{H}, \mathcal{A} \rangle$ is m-partite if we can partition the set of nodes $\mathcal{H}$ into m subsets $\mathcal{H}(1) \cdots \mathcal{H}(m)$, which we call *layers*, so that for each arc $i \in \mathcal{H}(h)$ and $j \in \mathcal{H}(h)$, $(i, j) \notin \mathcal{A}$. In the modelling framework introduced hereafter, $\mathcal{A}$ contains linkages across which power transmissions and losses occurs.

Contextually, we let $\mathcal{H}(1)$ be a collection of generation stations (*Genstat* from now on), with $|\mathcal{H}(1)| = n_1$; $\mathcal{H}(2) \cdots \mathcal{H}(m-1)$ be a collection of substations (*substat* from now on) from layer 1 up to layer $m-2$, with $|\mathcal{H}(2)| = n_2 \cdots |\mathcal{H}(m-2)| = n_{m-2}$; and $\mathcal{H}(m)$ be a collection of consumption centers (*Concent* from now on) at layer $m-1$, with $|\mathcal{H}(m)| = n_m$. Therefore, the electricity power is produced at generation stations; passes through substations, where its voltage is transformed; arrives at the last substations where its voltage is reduced; and is finally delivered to consumption centers for its domestic and/or industrial use. To distinguish substations from consumption centers and generators, we also define sets $\hat{\mathcal{H}} = \mathcal{H} \backslash \mathcal{H}(m)$ and $\mathcal{H}_I = \mathcal{H}(2) \cdots \mathcal{H}(m-1)$.

Let us define $i(a)$ and $j(a)$ as the left and right stations of line $a \in \mathcal{A}$, respectively. Then, the notations $a \in \mathcal{A}$, $(i(a), j(a)) \in \mathcal{A}$ and $(i, j) \in \mathcal{A}$ are interchangeably used. Next to it, we define a partition of $\mathcal{A}$ into a collection of working lines $\mathcal{A}^E$ and a collection of new possible lines $\mathcal{A}^N$ to be built. Finally, we create the

[3] Multi-period decisions on investments are not analyzed, as the Electricity and Co-generation Authority of Saudi Arabia establishes the annual budgets for the construction of new transmission lines and for the expansion of station capacities, looking at the annual level impact and without the possibility of spreading the budget along a longer time horizon.

subset of lines connecting generation stations to transmission stations $\mathcal{A}^G = \{(i,j) \in \mathcal{A} : i \in \mathcal{H}(1)\}$ for the ease of formulating terms related to power generation later on this section.

To tailor a well-suited mathematical programming model, integrating the above components, the following assumptions have been made:

- *Directional power flow.* We consider a directional power flow, from highest voltage stations to lowest voltage ones, proceeding downstream from left to right in the m-partite graph.
- *Power losses and recovery.* Uniform power losses are assumed for transmission lines between two points in the system and do not account for transitions sometimes incorporated into the network.[4] Losses are recovered by injecting reactive power using dedicated equipment.
- *Aggregate energy sources.* Motivated by the observation in the data set, the different energy sources are considered in aggregate production.[5]
- *End user aggregation.* Given the large number of consumers in the area under study, the local end users at each district have been aggregated to one point. This assumption is made to reduce the model size without affecting its functionality.
- *Uniform pricing within locations.* In most electricity markets prices vary for residential, commercial and industrial customers. We assume a unique price level for each consumption center.

The detailed model formulation for this described power system is presented in the next subsection.

3.2 Optimization model

The two-stage stochastic models presented hereafter relies on two types of first-stage decisions taken by the electricity company under demand uncertainty: (i) the electricity pricing for the consumption centers and (ii) the capacity expansion at each station and line level. We build our model by defining the profit structure of the electricity company and the collection of operational requirements restricting the company decisions. To do so, a list of decision variables and state variables (whose values are determined for each operator decision) are introduced below.

First-state decision variables:

μ_h	price variation at consumption center $h \in \mathcal{H}(m)$;
u_i	level of expansion of station $i \in \hat{\mathcal{H}}$;
z_a	binary decision for the creation of line $a \in \mathcal{A}^N$;

State variables:

x_a	power transmitted through line $a \in \mathcal{A}$;
$\mathcal{L}_a(x_a)$	loss from power transmitted through line $a \in \mathcal{A}$;
$r_{j(a)}$	power recovered at substation $j(a) \in \mathcal{H}_I$.
$\theta_{j(a)}$	current/voltage angles (phase difference) at station $j(a) \in \mathcal{H}_I$.[6]

[4] Such transitions (for instance, infrastructural or natural obstructions) have a minor impact on line losses.

[5] Fossil-based energy sources are the main energy source in SEC as the renewable sources represent only 0.2% of the total energy generation in Saudi Arabia (IRENA 2019). For that reason, energy storage stations are also disregarded.

[6] In AC circuits, the sinusoidal wave of the current and voltage magnitudes do not reach their maximum values at the same time. The fraction of a period difference between the maximum values is said to be the phase difference or nodal angles, representing state variables in optimal power flow models.

In vector form, let $\mathbf{x} \in \mathbb{R}^{|\mathcal{A}|}$ and $\mathbf{r} \in \mathbb{R}^{|\mathcal{H}_I|}$ be made of the x_a and r_j components respectively, and define $\mathbf{x}_i^+ \in \mathbb{R}^{|\mathcal{H}_I|}$ and $\mathbf{x}_i^- \in \mathbb{R}^{|\mathcal{H}_I|}$ as the corresponding vectors of energy inflow and outflow from $i \in \mathcal{H}_I$. The vectors for expansion decisions are $\mathbf{u} \in \mathbb{R}^{|\hat{\mathcal{H}}|}$ and $\mathbf{z} \in \mathbb{R}^{|\mathcal{A}^N|}$, respectively.

Using these variables, generation is defined as the total power flow produced in the first layer $\mathcal{H}(1)$, while the recovery at each substation is (lower and upper) bounded by fixed proportions ($\check{\rho}$ and $\hat{\rho}$) of the total loss from the incoming lines. Likewise Aussel et al. (2019), we assume that the electricity supplier influences the demand of the customers by setting prices. Defining P_h as the current price level and $\mu_h \in [-\hat{\mu}, \hat{\mu}] \subset [-1, 1]$ as a proportion of price adjustment at each consumption center $h \in \mathcal{H}(m)$, we consider the updated electricity price $P_h\,(1 + \mu_h)$. Similarly, by letting D_h be the expected demand at price P_h and ξ_h a random quantity (taking values between $\xi_{\min}$ and $\xi_{\max}$) at each consumption center $h \in \mathcal{H}(m)$, we define its electricity demand as $D_h(1 + \delta_h(\mu_h) + \xi_h)$, i.e., the current demand plus a shift induced by the price variation, where δ_h is a real-valued function mirroring the price sensitivity of demands.

Overall, the profit structure of the electricity company can be expressed as the revenue from real sales minus the aforementioned sources of costs using the following formula:

$$\text{Profit} \;:=\; \underbrace{\sum_{h \in \mathcal{H}(m)} P_h\,(1 + \mu_h)\,D_h\,(1 + \delta_h(\mu_h) + \xi_h)}_{R(\boldsymbol{\mu})} - \underbrace{C_g \sum_{a \in \mathcal{A}^G} x_a - C_r \sum_{j \in \mathcal{H}_I} r_j}_{T(\mathbf{x},\mathbf{r})} - \underbrace{\sum_{i \in \hat{\mathcal{H}}} e_i u_i}_{E_S(\mathbf{u})} - \underbrace{\sum_{a \in \mathcal{A}^N} \beta d_a z_a}_{E_L(\mathbf{z})}$$

where C_g and C_r are the generation and recovery costs (per KW), e_i is the unitary cost (per KW) for capacity expansion at station $i \in \hat{\mathcal{H}}$, d_a is the physical length of a line $a \in \mathcal{A}$ connecting station $i(a) \in \hat{\mathcal{H}}$ to station/consumption center $j(a) \in \mathcal{H}(m)$, and β is a proportionality constant.[7] Therefore, while the total revenue comes from the realized demand, the cost structure is made up with three terms corresponding to generation and recovery $T(\mathbf{x}, \mathbf{r})$, stations expansion $E_S(\mathbf{u})$, and line construction $E_L(\mathbf{z})$.

The resulting profit maximization problem (for centralized risk-neutral electricity companies) is formulated as a stochastic programming model, taking advantage of the fact that the probability distributions governing the demands are known:[8]

$$\hat{G}(\mathbf{C}, \boldsymbol{\rho}) = \begin{cases} \max\limits_{\mathbf{u},\mathbf{z},\boldsymbol{\mu}} & R(\boldsymbol{\mu}) - \mathbb{E}_{\boldsymbol{\xi}}\left[Q_{\boldsymbol{\xi}}(\boldsymbol{\lambda}; \mathbf{C}, \boldsymbol{\rho})\right] - E_S(\mathbf{u}) - E_L(\mathbf{z}) & \text{(1a)} \\ \text{subj. to} & P_h\,(1 + \mu_h) - P_{h'}\,(1 + \mu_{h'}) \le \Theta, \quad \text{for } h, h' \in \mathcal{H}(m) & \text{(1b)} \\ & \sum\limits_{a \in \mathcal{A}} \hat{z}_a \le B & \text{(1c)} \\ & \hat{f}_i - \hat{s}_i \ge u_i \ge 0, \quad \text{for } \; i \in \hat{\mathcal{H}} & \text{(1d)} \\ & \hat{\mu} \ge \mu_h \ge -\hat{\mu}, \quad \text{for } \; h \in \mathcal{H}(m) & \text{(1e)} \\ & z_a \in \{0, 1\}, \quad \text{for } \; a \in \mathcal{A}^N & \text{(1f)} \end{cases}$$

where $\boldsymbol{\lambda}^\top = [\boldsymbol{\mu}^\top \; \mathbf{u}^\top \; \mathbf{z}^\top]$ is the vector of first stage decisions, $Q_{\boldsymbol{\xi}}(\boldsymbol{\lambda}; \mathbf{C}, \boldsymbol{\rho})$ is a random variable (the generation and recovery cost) induced by $\boldsymbol{\xi}$, for any decision $\boldsymbol{\lambda}$, $\mathbb{E}_{\boldsymbol{\xi}}$ is the expectation operator with respect to the random

[7] We are assuming that the construction cost of lines is β (exogenous parameter) times the distance d_a between the stations to be connected (i.e., $\beta d_a z_a$). This parameter will be empirically calibrated for the computational experiments run in Section 7.

[8] Two-stage stochastic models have been applied in a broad range of areas ranging from production planning, scheduling problems, routing and transportation, and portfolio management. A general discussion on this class of problems is presented by Birge & Louveaux (2011).

term $\boldsymbol{\xi}$, and $\mathbf{C}^\top = [C_g\ C_r]$, $\boldsymbol{\rho}^\top = [\check{\rho}\ \hat{\rho}]$. Constraints (1b) impose a maximum variation on prices between pairs of consumption centers;[9] constraints (1c) set the maximum number of lines which can be potentially built, due to available expansion resources;[10] constraints (1d) limit the maximum expansion on station capacities given their upper and lower bounds $\hat{f}_i$ and $\hat{s}_i$; finally, constraints (1f)-(1e) set the variables domain.

Once the pricing and expansion decisions are taken, function $Q_{\boldsymbol{\xi}}(\boldsymbol{\lambda}; \mathbf{C}, \boldsymbol{\rho})$ (whose expectation is often called *recourse function*) is computed by finding the $\mathbf{x}$, $\boldsymbol{\theta}$ and $\mathbf{r}$ minimizing the generation and recovery costs and subject to a collection of physical laws involving the power flow going through the electricity grid. This problem can be written as a parameterized optimization model taking a realized demand noise $\boldsymbol{\xi}$ together with pricing and expansion decisions $\boldsymbol{\lambda}$ as inputs:

$$
Q_{\boldsymbol{\xi}}(\boldsymbol{\lambda}; \mathbf{C}, \boldsymbol{\rho}) = \left\{
\begin{array}{lll}
\max\limits_{\mathbf{x},\mathbf{r},\theta} & -C_g \sum\limits_{a \in \mathcal{A}^G} x_a - C_r \sum\limits_{j \in \mathcal{H}_I} r_j & \text{(2a)} \\
\text{subj. to} & (\mathbf{x}_h^+)^\top \mathbf{1} = D_h \left(1 + \delta_h(\mu_h) + \xi_h\right), \quad \text{for } h \in \mathcal{H}(m) & \text{(2b)} \\
& \left(\mathbf{x}_i^+ + r_i - \mathcal{L}(\mathbf{x}_i^-)\right)^\top \mathbf{1} = (\mathbf{x}_i^-)^\top \mathbf{1}, \quad \text{for } i \in \mathcal{H}_I & \text{(2c)} \\
& (\mathbf{x}_i^-)^\top \mathbf{1} \leq \hat{s}_i + u_i, \quad \text{for } i \in \hat{\mathcal{H}} & \text{(2d)} \\
& \check{\rho}\mathcal{L}(\mathbf{x}_i^-) \leq r_i \leq \hat{\rho}\mathcal{L}(\mathbf{x}_i^-), \quad \text{for } i \in \mathcal{H}_I & \text{(2e)} \\
& x_a = \gamma_a \sin(\theta_{i(a)} - \theta_{j(a)}), \quad \text{for } a \in \mathcal{A}^E & \text{(2f)} \\
& x_a = z_a \gamma_a \sin(\theta_{i(a)} - \theta_{j(a)}), \quad \text{for } a \in \mathcal{A}^N & \text{(2g)} \\
& |\theta_{i(a)} - \theta_{j(a)}| \leq \pi/4, \quad \text{for } a \in \mathcal{A}^E & \text{(2h)} \\
& |\theta_{i(a)} - \theta_{j(a)}| \leq (\pi/4) z_a, \quad \text{for } a \in \mathcal{A}^N & \text{(2i)} \\
& |x_a| \leq M z_a, \quad \text{for } a \in \mathcal{A}^N & \text{(2j)}
\end{array}
\right.
$$

where γ_a is the line conductance from station $i(a) \in \hat{\mathcal{H}}$ to station $j(a) \in \hat{\mathcal{H}}$. The objective function (2a) is the sum of generation and recovery costs.[11] Constraints (2b) ensure that the amount of electricity required by each consumption center is supplied; constraints (2c) enforce the flow balance at substations (Kirchhoff's first law); constraints (2d) limit the amount of outgoing power at stations;[12] constraints (2e) establish lower and

[9] The electricity tariffs for all categories of consumption are set by a governmental decree from the Saudi Council of Ministers, being reviewed on regular basis. There are a number of different determinants of the electricity prices, such as the oil price, government subsidies, local weather patterns, transmission and distribution infrastructure, among others. The last review of the electricity prices was made in 2017 and the latest tariffs were approved by the council on 12/12/2017 and applied starting from 1/1/2018. The decision taking process unfolds in two steps. Firstly, SEC propose a collection of price adjustment to the Saudi Council of Ministers. Secondly, the latter decide on the approval of the proposed prices. Indirectly, this procedure forces SEC to set prices which are likely to verify the regulatory requirements by the Saudi Council of Ministers (among which is the uniformity across locations).

[10] The decision of building a new line is governed by numerous technical constraints such as the availability of spare feeder at the corresponding station, the availability of reserve capacity to be fed to the line as well as the results of the line feasibility study conducted by the electricity company.

[11] Recovery is carried out based on local equipment at a rate comprised within $[\check{\rho}, \hat{\rho}]$ of the total loss from the incoming lines. The problem of finding the optimum location for introducing compensation has been already studied in the electrical engineering literature (Rajarman et al. 1998). Nowadays utilities tend to install this equipment in the proximity of the transmission point. Two main classes of compensation technologies can be considered: static technologies (such as capacitor bank, series compensator, shunt reactor and static synchronous compensator), as well as dynamic technologies (such as synchronous condenser). The main advantage of dynamic over static compensation schemes is their near-instantaneous response to changes in the system voltage. The power system studied in this paper is made up of dynamic compensation.

[12] Note that lines have no electricity limit since the excess of power flow is translated into losses through lines resistance.

upper bounds on power loss recovery with the aid of parameters $\check{\rho}$ and $\hat{\rho}$, respectively; constraints (2f)-(2g) represent the admittance matrix in polar coordinates to verify the Kirchhoff's second law on new possible lines and working lines;[13] constraints (2h) and (2i) force phase stability by requiring the absolute difference between phase angle of each node pair to be less than $\pi/4$.; Finally, constraints (2j) prevent the circulation of electricity flow in new transmission lines if not constructed.

Conventionally, $Q_{\boldsymbol{\xi}}(\boldsymbol{\lambda}; \mathbf{C}, \boldsymbol{\rho})$ takes value minus infinite when pricing and expansion decisions are not feasible for all the possible realizations of the random demands, requiring $\boldsymbol{\lambda}$ to be feasible for any realization of $\boldsymbol{\xi}$. As discussed by Birge & Louveaux (2011), when modeling daily or hourly power demand, focus is on the system reliability. For this reason, alternative technologies (called a *backstop* technologies) can be embedded in the system and formulated in the model by expressing a minimum probability for meeting demands using the non-backstop technologies (known as *probabilistic constraints*). Looking at average demands over the annual period (see Section 6) allows circumventing the hourly and daily fluctuations of the power demand, while capturing a stable behavior for the purpose of price setting and capacity expansion.

3.3 Linearization

The two-stage stochastic model (1) is a non-linear and non-convex optimization problem containing different sources of non-linearities: the nonlinear revenue term $R(\boldsymbol{\mu})$ in (1a), the sinusoidal terms in constraints (2f)-(2g), and the functional form of $\mathcal{L}$ characterizing power losses. This subsection addresses the linearization of all these terms, resulting in a MILP approximating the original power flow model.

The linearized revenue. The revenue function $R(\boldsymbol{\mu})$ is a non-linear function due to the term $\mu_h \delta_h(\mu_h)$. We proposed a linearization strategy based on a discretized collection of price increments $\mathcal{P}^+$ and price decrements $\mathcal{P}^-$ per KW with respect to the current price level P_h, along with the following decision variables:

w^+_{ph} binary decision for a price increase of level $p \in \mathcal{P}^+$ at consumption center $h \in \mathcal{H}(m)$;
w^-_{ph} binary decision for a price decrease of level $p \in \mathcal{P}^-$ at consumption center $h \in \mathcal{H}(m)$;

This discretization strategy often reflects the actual price adjustment policy, where a finite collection of increments or decrements are proposed to the public authority by the electricity company. The discrete approximation of price levels and associated demands are respectively defined as

$$\mu_h \approx \sum_{p \in \mathcal{P}^+} \mu^+_{ph} w^+_{ph} - \sum_{p \in \mathcal{P}^-} \mu^-_{ph} w^-_{ph} \qquad \text{and} \qquad \delta_h(\mu_h) \approx -\sum_{p \in \mathcal{P}^+} \phi^+_{ph} w^+_{ph} + \sum_{p \in \mathcal{P}^-} \phi^-_{ph} w^-_{ph} \tag{3}$$

under the condition

$$\sum_{p \in \mathcal{P}^+} w^+_p + \sum_{p \in \mathcal{P}^-} w^-_p \leq 1. \tag{4}$$

where the parameters μ^+_{ph} and μ^-_{ph} denote predefined price increments and decrements (expressed as a proportion of the current price P_h), respectively; while ϕ^+_{ph} and ϕ^-_{ph} are the corresponding demand increase and decrease

Conversely, as extensively described in Section 7, the inclusion of stations capacities relies on the availability of annual demand at consumption centers. Therefore, station capacities can be directly imposed, rather than probabilistic constrains to prevent persistent excess of power flow at the daily or hourly based demand (see Birge & Louveaux (2011) for more details on the use of probabilistic constraints for capacity expansion in power systems).

[13] This formulation assumes that the line reactance is much smaller compared to the line resistance. This assumption is valid for low transmission frequencies (around 50 Hertz), which are proportional to the reactance value.

from the price variation, respectively (expressed as a proportion of the current demand D_h). From (3)-(4), we obtain:

$$\begin{aligned} R(\mu_h) &\approx P_h D_h \Big(1 + \sum_{p\in\mathcal{P}^+} \mu^+_{ph} w^+_{ph} - \sum_{p\in\mathcal{P}^-} \mu^-_{ph} w^-_{ph}\Big)\Big(1 - \sum_{p\in\mathcal{P}^+} \phi^+_{ph} w^+_{ph} + \sum_{p\in\mathcal{P}^-} \phi^-_{ph} w^-_{ph} + \xi_h\Big) \\ &= P_h D_h \Big(\sum_{p\in\mathcal{P}^+} \kappa^+_{ph} w^+_{ph}\Big) - P_h D_h \Big(\sum_{p\in\mathcal{P}^-} \kappa^-_{ph} w^-_{ph} + \xi_h\Big) + P_h D_h \\ &= P_h D_h \Big(\sum_{p\in\mathcal{P}^+} \kappa^+_{ph} w^+_{ph} - \sum_{p\in\mathcal{P}^-} \kappa^-_{ph} w^-_{ph}\Big) + S_\xi \end{aligned} \tag{5}$$

where $\kappa^+_{ph} = \mu^+_{ph}(1 - \phi^+_{ph} + \xi_h) - \phi^+_{ph}$ and $\kappa^-_{ph} = \mu^-_{ph}(1 - \phi^-_{ph} + \xi_h) - \phi^-_{ph}$ are exogenous parameters obtained by factorizing the demand sensitivity coefficients with the price variations and $S_\xi = \sum_{h\in\mathcal{H}(m)} P_h D_h (1 + \xi_h)$.

The linearized Kirchhoff's second law. As assumed in the main literature, DC power flow problems (Romero et al. 2002, Alguacil et al. 2003, Correa-Florez et al. 2014, Jenabi et al. 2015) can approximate the power flow model (2) under normal operating conditions, in which the difference between the nodal angles prevailing at lines extremes is small enough. This is enforced by stability constraints (2h) and (2i), as suggested by Jenabi et al. (2015). Based on these constraints and the use of recovery equipment injecting reactive power for the losses recovery, the sinusoidal components in (2f)-(2g) can be linearized as $\sin(\theta_i - \theta_j) \approx \theta_i - \theta_j$. By replacing the product between binary and continuous variables with the aid of additional constraints, we linearize (2f)-(2h) as follows:

$$x_a = \gamma_a(\theta_{i(a)} - \theta_{j(a)}), \qquad \text{for } a \in \mathcal{A}^E \tag{2e-lin}$$

$$x_a \le \gamma_a(\theta_{i(a)} - \theta_{j(a)}) + M(1 - z_a), \qquad \text{for } a \in \mathcal{A}^N \tag{2f-lin-ub}$$

$$x_a \ge \gamma_a(\theta_{i(a)} - \theta_{j(a)}) - M(1 - z_a), \qquad \text{for } a \in \mathcal{A}^N \tag{2f-lin-lb}$$

$$\pi/4 \le \theta_{i(a)} - \theta_{j(a)}, \qquad \text{for } a \in \mathcal{A}^E \tag{2g-lin-ub}$$

$$\pi/4 \ge \theta_{i(a)} - \theta_{j(a)}, \qquad \text{for } a \in \mathcal{A}^E \tag{2g-lin-lb}$$

$$(\pi/4)z_a \le \theta_{i(a)} - \theta_{j(a)}, \qquad \text{for } a \in \mathcal{A}^N \tag{2h-lin-ub}$$

$$(\pi/4)z_a \ge \theta_{i(a)} - \theta_{j(a)}, \qquad \text{for } a \in \mathcal{A}^N \tag{2h-lin-lb}$$

where M is a sufficiently large value (i.e., larger than the maximum power flow that can pass though the line).

The linearized loss function. The functional form of $\mathcal{L}$ constitutes another source of non-linearity in the model, induced also from a sinusoidal function of the difference between nodal angles at the line extremes. Based on a second order approximation of the cosine function, and using the already mentioned linearization of the Kirchhoff's second law (2f)-(2g), Alguacil et al. (2003) describe the power losses as:

$$\mathcal{L}_a(x_a) = \varepsilon_a \left[1 - \cos(\theta_{i(a)} - \theta_{j(a)})\right] \approx \varepsilon_a(\theta_{i(a)} - \theta_{j(a)})^2 = \frac{\varepsilon_a}{\gamma_a^2}(x_a)^2. \tag{6}$$

where ε_a is the line susceptance from station $i(a) \in \hat{\mathcal{H}}$ to station $j(a) \in \hat{\mathcal{H}}$. This quadratic form can be approached from below by a piece-wise linear approximation[14], inducing a model relaxation that can be made

[14] As stated in (Krasko & Rebennack 2017), piece-wise linear approximations (see, for instance, Rebennack & Kallrath (2015)) and their representation (Vielma & Nemhauser 2011) have not been fully utilized for power flow models, while they have a successful story for another network transmission problem such us gas pipeline transportation (see, for instance Fügenschuh et al. (2014)).

arbitrarily close to the original feasible region by increasing the number of linear cuts.[15] Hereafter, we consider T pivot nodes and define a Taylor expansion of $\mathcal{L}_a(x_a)$ around $\hat{x}_{a,1} \dots \hat{x}_{a,T}$. The power losses on line a can be bounded from below as:

$$\mathcal{L}_a(x_a) \;=\; \frac{\varepsilon_a}{\gamma_a^2}(x_a)^2 \;\geq\; \max_t \left\{ \frac{\varepsilon_a}{\gamma_a^2}(\hat{x}_{a,t})^2 + 2\frac{\varepsilon_a}{\gamma_a^2}(\hat{x}_{a,t})(x_a - \hat{x}_{a,t}) \right\} \tag{7}$$

Note that, the piece-wise linear function coincides with the actual power losses function in the pivots $\hat{x}_{a,1} \dots \hat{x}_{a,T}$; whereas, the maximum deviation values are in the knots $\hat{x}^0_{a,1} \dots \hat{x}^0_{a,T}$.

The linearized two-stage stochastic problem. Using (5), (2e-lin)-(2h-lin-lb) and (7), a linearized version of (2a)–(2j) can be written as:

$$\hat{Q}_{\boldsymbol{\xi}}(\boldsymbol{\lambda}; \mathbf{C}, \boldsymbol{\rho}) = \begin{cases} \max\limits_{\mathbf{x},\mathbf{r},\ell,\theta} & -C_g \sum\limits_{a \in \mathcal{A}^G} x_a - C_r \sum\limits_{j \in \mathcal{H}_I} r_j & & \text{(8a)} \\ \text{s.t.} & (\mathbf{x}_h^+)^\top \mathbf{1} = D_h \left(1 - \boldsymbol{\phi}_h^\top \mathbf{w}_h + \xi_h\right), & \text{for } h \in \mathcal{H}(m) & \text{(8b)} \\ & \left(\mathbf{x}_i^+ + r_i - \sum\limits_{a \in \mathcal{A}_i^+} \ell_a\right)^\top \mathbf{1} = (\mathbf{x}_i^-)^\top \mathbf{1}, & \text{for } i \in \mathcal{H}_I & \text{(8c)} \\ & (\mathbf{x}_i^-)^\top \mathbf{1} \leq \hat{s}_i + u_i, & \text{for } i \in \hat{\mathcal{H}} & \text{(8d)} \\ & \check{\rho} \sum\limits_{a \in \mathcal{A}_i^+} \ell_a \leq r_i \leq \hat{\rho} \sum\limits_{a \in \mathcal{A}_i^+} \ell_a, & \text{for } i \in \mathcal{H}_I & \text{(8e)} \\ & x_a = \gamma_a(\theta_{i(a)} - \theta_{j(a)}), & \text{for } a \in \mathcal{A}^E & \text{(8f)} \\ & x_a \leq \gamma_a(\theta_{i(a)} - \theta_{j(a)}) + M(1 - z_a), & \text{for } a \in \mathcal{A}^N & \text{(8g)} \\ & x_a \geq \gamma_a(\theta_{i(a)} - \theta_{j(a)}) - M(1 - z_a), & \text{for } a \in \mathcal{A}^N & \text{(8h)} \\ & \ell_a \geq 2\frac{\varepsilon_a}{\gamma_a^2}(\hat{x}_{a,t})x_a - \frac{\varepsilon_a}{\gamma_a^2}(\hat{x}_{a,t})^2, & \text{for } a \in \mathcal{A},\ t \in \mathcal{T} & \text{(8i)} \\ & -\pi/4 \leq \theta_{i(a)} - \theta_{j(a)} \leq \pi/4, & \text{for } a \in \mathcal{A}^E & \text{(8j)} \\ & -(\pi/4)z_a \leq \theta_{i(a)} - \theta_{j(a)} \leq (\pi/4)z_a, & \text{for } a \in \mathcal{A}^N & \text{(8k)} \end{cases}$$

while the first stage problem becomes

$$\hat{G}(\mathbf{C}, \boldsymbol{\rho}) = \begin{cases} \max\limits_{\mathbf{u},\mathbf{z},\mathbf{w}} & \sum\limits_{h \in \mathcal{H}(m)} P_h D_h \boldsymbol{\kappa}_h^\top \mathbf{w}_h - \mathbb{E}_{\boldsymbol{\varepsilon}}\left[\hat{Q}_{\boldsymbol{\xi}}(\boldsymbol{\lambda}; \mathbf{C}, \boldsymbol{\rho})\right] - E_S(\mathbf{u}) - E_L(\mathbf{z}) & & \text{(9a)} \\ \text{s.t.} & P_h \boldsymbol{\mu}_h^\top \mathbf{w}_h - P_{h'} \boldsymbol{\mu}_{h'}^\top \mathbf{w}_{h'} \leq \hat{\Theta}_{h,h'}, & \text{for } h, h' \in \mathcal{H}(m), & \text{(9b)} \\ & \mathbf{w}_h^\top \mathbf{1} \leq 1, & \text{for } h \in \mathcal{H}(m) & \text{(9c)} \\ & \mathbf{z}^\top \mathbf{1} \leq B & & \text{(9d)} \\ & \mathbf{z}, \mathbf{w}, \mathbf{u} \;\text{ verifying the variable bounds} & & \text{(9e)} \end{cases}$$

[15] Note that the intrinsic difficulty in solving that problem using standard MILP techniques might increase substantially with the number of approximation lines, thus the resulting trade-off between accuracy and performance must be considered. (See Section 7 for a numerical analysis of this aspect.)

where we redefined $\hat{\Theta}_{h,h'} = \Theta + P_{h'} - P_h$ and dropped the term S_ξ from the revenue, as it is a constant with respect to the problem variables. Therefore, $G(\mathbf{C}, \boldsymbol{\rho}) \approx \hat{G}(\mathbf{C}, \boldsymbol{\rho}) + S_\xi$. We also introduced the vector notation $\boldsymbol{\kappa}_h, \mathbf{w}_h, \boldsymbol{\phi}_h, \boldsymbol{\mu}_h \in \mathbb{R}^{|\mathcal{P}^+|+|\mathcal{P}^-|}$, containing the components of κ^+_{ph}, κ^-_{ph}; w^+_{ph}, w^-_{ph}; ϕ^+_{ph}, ϕ^-_{ph}; and μ^+_{ph}, μ^-_{ph}. Constraints (9b) are the linearized version of (1c), which are enforced by (9c), setting the selection of a unique pricing policy.

The multi-scenario formulation. The two-stage stochastic problem (9)-(8), has still a remaining source of non-linearity, driven by the implicitly defined recourse function $\hat{Q}_{\boldsymbol{\xi}}(\boldsymbol{\lambda}; \mathbf{C}, \boldsymbol{\rho})$. Under very specific cases (as explored in Section 4) this problem can be analytically solved, by the algebraic characterization of the functional form of $\hat{Q}_{\boldsymbol{\xi}}(\boldsymbol{\lambda}; \mathbf{C}, \boldsymbol{\rho})$. However, for its general solvability, two-stage stochastic problem (8)-(9) can be approximated (with arbitrary precision) by a mixed-integer linear program by means of a finite realization of $\boldsymbol{\xi}$ (often referred to as *scenarios*): $\boldsymbol{\xi}_1 \dots \boldsymbol{\xi}_S$, with associated probabilities $\pi_1 \dots \pi_S$. We denote with $\mathcal{S}$ the collection of indexes corresponding to the S scenarios and consider the following deterministic equivalent problem:

$$
\left\{
\begin{array}{lll}
\max\limits_{\mathbf{u},\mathbf{z},\mathbf{w},\mathbf{x},\mathbf{r},\ell,\theta} & \sum\limits_{s\in\mathcal{S}} \pi_s \left[\sum\limits_{h\in\mathcal{H}(m)} P_h D_h \boldsymbol{\kappa}_h^\top \mathbf{w}_h - C_g \sum\limits_{a\in\mathcal{A}^G} x_{as} - C_r \sum\limits_{j\in\mathcal{H}_I} r_{js} \right] & -E_S(\mathbf{u}) - E_L(\mathbf{z}) \\
\text{s.t.} & (\mathbf{x}^+_{hs})^\top \mathbf{1} = D_h \left(1 - \boldsymbol{\phi}_h^\top \mathbf{w}_h + \xi_{hs}\right), & \text{for } h \in \mathcal{H}(m),\ s \in \mathcal{S} \\
& \left(\mathbf{x}^+_{is} + r_{is} - \sum\limits_{a\in\mathcal{A}^+_i} \ell_{as}\right)^\top \mathbf{1} = (\mathbf{x}^-_{is})^\top \mathbf{1}, & \text{for } i \in \mathcal{H}_I,\ s \in \mathcal{S} \\
& (\mathbf{x}^-_{is})^\top \mathbf{1} \le \hat{s}_i + u_i, & \text{for } i \in \hat{\mathcal{H}},\ s \in \mathcal{S} \\
& \check{\rho} \sum\limits_{a\in\mathcal{A}^+_i} \ell_{as} \le r_{is} \le \hat{\rho} \sum\limits_{a\in\mathcal{A}^+_i} \ell_{as}, & \text{for } i \in \mathcal{H}_I,\ s \in \mathcal{S} \\
& x_{as} = \gamma_a(\theta_{i(a)s} - \theta_{j(a)s}), & \text{for } a \in \mathcal{A}^E,\ s \in \mathcal{S} \\
& x_{as} \le \gamma_a(\theta_{i(a)s} - \theta_{j(a)s}) + M(1 - z_a), & \text{for } a \in \mathcal{A}^N,\ s \in \mathcal{S} \\
& x_{as} \ge \gamma_a(\theta_{i(a)s} - \theta_{j(a)s}) - M(1 - z_a), & \text{for } a \in \mathcal{A}^N,\ s \in \mathcal{S} \\
& \ell_{as} \ge 2\frac{\varepsilon_a}{\gamma_a^2}(\hat{x}_{ats}) x_{as} - \frac{\varepsilon_a}{\gamma_a^2}(\hat{x}_{ats})^2, & \text{for } a \in \mathcal{A},\ t \in \mathcal{T} \\
& P_h \boldsymbol{\mu}_h^\top \mathbf{w}_h - P_{h'} \boldsymbol{\mu}_{h'}^\top \mathbf{w}_{h'} \le \hat{\Theta}_{h,h'}, & \text{for } h, h' \in \mathcal{H}(m), \\
& \mathbf{w}_h^\top \mathbf{1} \le 1, & \text{for } h \in \mathcal{H}(m) \\
& \mathbf{z}^\top \mathbf{1} \le B & \\
& z_a \in \{0,1\}, & \text{for } a \in \mathcal{A}^N \\
& w^+_{ph} \in \{0,1\}, & \text{for } p \in \mathcal{P}^+,\ h \in \mathcal{H} \\
& w^-_{ph} \in \{0,1\}, & \text{for } p \in \mathcal{P}^-,\ h \in \mathcal{H} \\
& \hat{f}_i - \hat{s}_i \ge u_i \ge 0, & \text{for } i \in \mathcal{H} \backslash \mathcal{H}(m) \\
& (\pi/4) \ge \theta_{i(a)s} - \theta_{j(a)s} \ge -(\pi/4), & \text{for } a \in \mathcal{A}^E \\
& (\pi/4) z_a \ge \theta_{i(a)s} - \theta_{j(a)s} \ge -(\pi/4) z_a, & \text{for } a \in \mathcal{A}^N
\end{array}
\right. \tag{10}
$$

The final MILP (10) involves $(|\mathcal{P}^+|+|\mathcal{P}^-|)|\mathcal{H}(m)|+|\mathcal{A}^N|$ binary variables and $|\mathcal{S}|(2|\mathcal{A}|+|\hat{\mathcal{H}}|)+\sum_{i=1}^{m-1}|\mathcal{H}(i)|$ continuous variables. A solution procedure for this large MILP is proposed in Section 5, based on a bounding approach which exploits the cost and revenue structure to build valid inequalities.

4 Illustrative cases of integrated planning

The modeling standpoints of this work is the substitutability among integrated decisions on electricity prices and expansion in centralized power systems, based on the different behaviours of the scaling cost induced by power losses. In this subsection, we consider four stylized cases in which this intricate substitution pattern can be analytically assessed.

Let P and D be the current price level and expected demand, respectively. The following notation is adopted throughout this section:

$$A = D(1+\mathbb{E}[\xi])(P - C_g), \qquad A^- = A - D(P\kappa^- + C_g\phi^-), \qquad A^+ = A + D(P\kappa^+ + C_g\phi^+)$$

along with $\hat{\xi} = \mathbb{E}[\xi]$ and $\xi_{\max} = \max\{\xi_1 \dots \xi_S\}$. The details of the algebraic development of the four examples presented in this Section are reported in Appendix A.

4.1 Power system with two generators and one consumption center

Consider a power system with two generators and no transaction station, i.e., $m = 2$, $\mathcal{H}(1) = \{1, 2\}$, $\mathcal{H}(2) = \{3\}$, so that $\mathcal{A}^E = \{(1, 3)\}$ and $\mathcal{A}^N = \{(2, 3)\}$. The following two examples provide closed-form solutions for the optimal price and expansion in this small system, under two different assumptions on the behaviour of power losses.

Example 1. *Let us assume $\check{\rho} = \hat{\rho} = 1$ and $C_g = C_r$. We assume that the activation of the second generator (and its corresponding line) is endogenously decided by setting the binary variable z, with a fix cost βd. Using the quadratic approximation (6), the optimal expected profit when prices are fixed is*

$$\begin{cases} A - C_g D^2 \mathbb{E}[(1+\xi)^2]\dfrac{\varepsilon_1}{\gamma_1^2} & \text{if } z = w^+ = w^- = 0 \\ A - C_g D^2 \mathbb{E}[(1+\xi)^2]\Xi_0 - \beta d & \text{if } z = 1,\ w^+ = w^- = 0 \end{cases}$$

and when prices are endogenously decided is

$$\begin{cases} A^- - C_g D^2 \mathbb{E}[(1+\phi^- +\xi)^2]\dfrac{\varepsilon_1}{\gamma_1^2} & \text{if } z = w^+ = 0,\ w^- = 1 \\ A^+ - C_g D^2 \mathbb{E}[(1-\phi^+ +\xi)^2]\dfrac{\varepsilon_1}{\gamma_1^2} & \text{if } z = w^- = 0,\ w^+ = 1 \\ A^- - C_g D^2 \mathbb{E}[(1+\phi^- +\xi)^2]\Xi_0 - \beta d & \text{if } w^+ = 0,\ z = w^- = 1 \\ A^+ - C_g D^2 \mathbb{E}[(1-\phi^+ +\xi)^2]\Xi_0 - \beta d & \text{if } w^- = 0,\ z = w^+ = 1 \end{cases}$$

where $\Xi_0 = \frac{\varepsilon_2}{\gamma_2^2} + (\frac{\varepsilon_2}{\gamma_2^2})^2(\frac{\varepsilon_1}{\gamma_1^2} - \frac{\varepsilon_2}{\gamma_2^2})(\frac{\varepsilon_1}{\gamma_1^2} + \frac{\varepsilon_2}{\gamma_2^2})^{-1}$. The following list details the optimal policy for the described power system.

- *When $\Xi_0 > \dfrac{\varepsilon_1}{\gamma_1^2}$, the activation of the second generator can never be profitable.*
- *When the electricity price is kept at the current level, if $\dfrac{\varepsilon_1}{\gamma_1^2} > \Xi_0 + \beta d/(C_g D^2 \mathbb{E}[(1+\xi)^2])$ then the activation of the second generator is profitable.*
- *When the electricity price is increased by $100(\phi^+)$ percent, if $\dfrac{\varepsilon_1}{\gamma_1^2} > \Xi_0 + \beta d/(C_g D^2 \mathbb{E}[(1-\phi^+ +\xi)^2])$ then the activation of the second generator is profitable.*
- *When the electricity price is reduced by $100(\phi^-)$ percent, if $\dfrac{\varepsilon_1}{\gamma_1^2} > \Xi_0 + \beta d/(C_g D^2 \mathbb{E}[(1+\phi^- +\xi)^2])$ then the activation of the second generator is profitable.*

Example 2. *Let us assume $\check{\rho} = \hat{\rho} = 0$. We assume that the substation capacity can be expanded with a unitary cost of e monetary units per KW. Using the quadratic approximation (6), the optimal expected profit when prices are fixed is*

$$\begin{cases} PD(1+\hat{\xi}) - C_g \dfrac{\gamma_1^2}{2\varepsilon_1}\left(1 - R(1,0)\right) & \text{if } z = w^+ = w^- = 0 \\ PD(1+\hat{\xi}) - C_g \left[\dfrac{\gamma_1^2}{2\varepsilon_1}\left(1 - R(\Xi_1,0)\right) + \dfrac{\gamma_2^2}{2\varepsilon_2}\left(1 - R(1-\Xi_1,0)\right)\right] - \beta d & \text{if } z = 1,\ w^+ = w^- = 0 \end{cases}$$

and when prices are endogenously decided is

$$\begin{cases} PD(1-\kappa^- + \hat{\xi}) - C_g \dfrac{\gamma_1^2}{2\varepsilon_1}\left(1 - R(1,\phi^+)\right) & \text{if } z = w^+ = 0,\ w^- = 1 \\ PD(1+\kappa^+ + \hat{\xi}) - C_g \dfrac{\gamma_1^2}{2\varepsilon_1}\left(1 - R(1,-\phi^-)\right) & \text{if } z = w^- = 0,\ w^+ = 1 \\ PD(1-\kappa^- + \hat{\xi}) - C_g \left[\dfrac{\gamma_1^2}{2\varepsilon_1}\left(1 - R(\Xi_1,\phi^+)\right) + \dfrac{\gamma_2^2}{2\varepsilon_2}\left(1 - R(1-\Xi_1,\phi^+)\right)\right] - \beta d & \text{if } w^+ = 0,\ z = w^- = 1 \\ PD(1+\kappa^+ + \hat{\xi}) - C_g \left[\dfrac{\gamma_1^2}{2\varepsilon_1}\left(1 - R(\Xi_1,-\phi^-)\right) + \dfrac{\gamma_2^2}{2\varepsilon_2}\left(1 - R(1-\Xi_1,-\phi^-)\right)\right] - \beta d & \text{if } w^- = 0,\ z = w^+ = 1 \end{cases}$$

where $\Xi_1 = \frac{\varepsilon_2}{\gamma_2^2}\left(\frac{\varepsilon_1}{\gamma_1^2} + \frac{\varepsilon_2}{\gamma_2^2}\right)^{-1}$ and $R(a,b) = \mathbb{E}[(1 - 4\frac{\varepsilon_2}{\gamma_2^2} aD(1+b+\xi))^{1/2}]$. Below, we list some properties of the optimal pricing and expansion policy for the described power system.

- *When the second generator is not activated, the pricing decision depends on the demand distribution and sensitivity ϕ^+ and ϕ^-, as well as on the conductance and susceptance of the first line.*
- *When the second generator is activated, the pricing decision depends on the demand distribution and sensitivity ϕ^+ and ϕ^-, as well as on the conductance and susceptance of both lines.*
- *The expansion decision is mainly driven by counter-effects of Ξ_1 and βd.*

Both examples reveal that the optimality of price variation and expansion strongly depends on the specific form of the scaling cost induced by power losses. In the first example, the presence of the new line (associated to the second generator) gives rise to a switch in the impact of the demand sensitivity ϕ^+ and ϕ^- on the optimal pricing policy. In the second example, since losses are not recovered the price decrease is never a profitable option, as a higher demand gives rise to non-compensated losses.

4.2 Power system with one generators, one transaction substation and one consumption center

Consider a power system with one generator, a transaction substation and a consumption center, i.e., $m = 3$, $\mathcal{H}(1) = \{1\}$, $\mathcal{H}(2) = \{2\}$ and $\mathcal{H}(3) = \{3\}$, so that $\mathcal{A}^E = \{(1,3),(2,3)\}$ and $\mathcal{A}^N = \varnothing$. The following two example provide closed-form solutions for the optimal price and expansion in this small system, under two different assumption on the behaviour of power losses.

Example 3. *We assume that $\check{\rho} = \hat{\rho} = 1$ and $C_g = C_r$ and that the substation capacity can be expanded with a unitary cost of e monetary units per KW. Using the quadratic approximation of power losses (6), the optimal expected profit for this power system when prices are fixed is:*

$$A - C_g D^2 \mathbb{E}[(1+\xi)^2]\left(\frac{\varepsilon_1}{\gamma_1^2} + \frac{\varepsilon_2}{\gamma_2^2}\right) - e(D(1+\xi_{\max}) - \hat{s})$$

and when prices are endogenously decided is

$$\begin{cases} A^- - C_g D^2 \mathbb{E}[(1+\phi^- + \xi)^2] \left(\frac{\varepsilon_1}{\gamma_1^2} + \frac{\varepsilon_2}{\gamma_2^2}\right) - e(D(1+\phi^- + \xi_{\max}) - \hat{s}) & \text{if } w^+ = 0,\ w^- = 1 \\ A^+ - C_g D^2 \mathbb{E}[(1-\phi^+ + \xi)^2] \left(\frac{\varepsilon_1}{\gamma_1^2} + \frac{\varepsilon_2}{\gamma_2^2}\right) - e(D(1-\phi^+ + \xi_{\max}) - \hat{s}) & \text{if } w^+ = 1,\ w^- = 0 \end{cases}$$

In this case, while higher-order moments of ξ have a negative impact on the profit with sensitivity $C_g D^2(\frac{\varepsilon_1}{\gamma_1^2} + \frac{\varepsilon_2}{\gamma_2^2})$, the optimal pricing policy is not sensitive to the right-tail of the demand distribution. We see that when losses are fully recovered, an increase in the unitary cost of substation expansion makes the electricity price reduction become less profitable on average.

Example 4. *We assume that $\check{\rho} = \hat{\rho} = 0$ and that the substation capacity can be expanded with a unitary cost of e monetary units per KW. Using the quadratic approximation of power losses (6), the optimal expected profit for this power system when prices are fixed is:*

$$A - C_g \left[4 - 8\frac{\varepsilon_2}{\gamma_2^2} T(\hat{\xi}) - \frac{1}{2} S(0) + (\Xi_1 - 1) R(0)\right] - e[T(\xi_{\max}) - \hat{s}]$$

and when prices are endogenously decided is

$$\begin{cases} A^+ - C_g \left[4 - 8\frac{\varepsilon_2}{\gamma_2^2} T(\hat{\xi} - \phi^-) - \frac{1}{2} S(-\phi^-) + (\Xi_1 - 1) R(-\phi^-)\right] - e[T(\xi_{\max} - \phi^-) - \hat{s}] & \text{if } w^+ = 1,\ w^- = 0 \\ A^- - C_g \left[4 - 8\frac{\varepsilon_2}{\gamma_2^2} T(\hat{\xi} + \phi^+)] - \frac{1}{2} S(\phi^+) + (\Xi_1 - 1) R(\phi^+)\right] - e[T(\xi_{\max} + \phi^+) - \hat{s}] & \text{if } w^+ = 0,\ w^- = 1 \end{cases}$$

where $\Xi_1 = \frac{\varepsilon_2}{\gamma_2^2} \left(\frac{\varepsilon_1}{\gamma_1^2} + \frac{\varepsilon_2}{\gamma_2^2}\right)^{-1}$ *and*

$$T(a) = D(1+a), \qquad R(a) = \mathbb{E}\left[\sqrt{1 - 4\frac{\varepsilon_2}{\gamma_2^2} T(a+\xi)}\right], \qquad S(a) = \mathbb{E}\left[\sqrt{1 - 2\Xi_1 \left(\sqrt{1 - 4\frac{\varepsilon_2}{\gamma_2^2} T(a+\xi)} - 1\right)}\right]$$

In this case, the sensitivity on profit of higher-order moments is $8 C_g D \frac{\varepsilon_2}{\gamma_2^2}$, the optimal pricing policy is not sensitive to the right-tail of the demand distribution. Hence, in the case of non recovered losses, within a certain rage the optimal pricing policy is poorly sensitive to the unitary cost of substation expansion (i.e. in the interval in which they are sufficiently low).

Also in this second illustrative power system, both examples reveal that the optimality of price variation and expansion strongly depends on the specific form of the scaling cost induced by power losses, unfolding at the second-stage problem.

5 Solution method

Apart from the stylized cases studied in Section 4, the resolution of (10) for real electricity markets requires the application of efficient algorithmic strategies. As explained by Krasko & Rebennack (2017), the use of bounding approaches on optimal power flow problems is a promising direction that has already given rise to good results (Frank & Rebennack 2015). Likewise, the use of piecewise-linear approximations, which have not been fully utilized for the OPF (Vielma & Nemhauser 2011, Rebennack & Kallrath 2015), have shown a success story in a wide range of applications (Rebennack & Krasko 2019) and particularly in related network transmission problems (Fügenschuh et al. 2014, López-Ramos et al. 2019).

Contextually, this section proposes a solution approach that relies on the efficient computation of lower and upper bounds to (10), supporting the selection of well-fitted pivots for the PWL approximation (6). As discussed in Subsection 3.2, let us consider the Taylor expansion of $\mathcal{L}_a(x_a)$ around $\hat{x}_{a,1} \dots \hat{x}_{a,T}$. The following proposition quantifies the approximation error for uniformly distributed pivots.

Proposition 1 (Goodness of piece-wise linear approximation)**.** *Consider two lists of pivots represented by the sequence* $\{\hat{x}_{a,0} + \tau t\}_{t=0}^{T}$*, for some* $\tau \in [0,1]$*, being* $\hat{x}_{a,0}$ *a starting pivot. For any* $x \in [\hat{x}_{a,1}, \hat{x}_{a,T}]$*, we have*

$$\mathcal{L}_a(x_a) - \max_{t \in \mathcal{T}} \left\{ \frac{\varepsilon_a}{\gamma_a^2}(\hat{x}_{a,t})^2 + 2\frac{\varepsilon_a}{\gamma_a^2}(\hat{x}_{a,t})(x_a - \hat{x}_{a,t}) \right\} \leq 4\frac{\varepsilon_a}{\gamma_a^2}\hat{x}_{a,0} \tag{11}$$

Proposition 1 points out that the maximum error within the approximation range $[\hat{x}_{a,1}, \hat{x}_{a,T}]$ is driven by the location of the starting pivot, which is unknown prior to the resolution of (10).

Coherently, to avoid the arbitrary selection of $\hat{x}_{a,0}$, the procedural steps below describes a solution method that avoids the uninformed selection, by using the information from a relaxed problem, where an *ideal power flow* in the absence of losses is estimated. Hence, we set up the case of fully recovered losses at zero cost (i.e., $\check{\rho} = \hat{\rho} = 1$ and $C_r = 0$), so that variables $\boldsymbol{\ell}$ can be eliminated from (10), resulting in the following linear programming computable recourse function:

$$\hat{Q}_\xi(\boldsymbol{\lambda}; [C_g\ 0], [1\ 1]) = \begin{cases} \max\limits_{\mathbf{x},\theta} & -C_g \sum\limits_{h \in \mathcal{H}(m)} D_h \left(1 - \boldsymbol{\phi}_h^\top \mathbf{w}_h + \xi_{hs}\right) & \\ \text{s.t.} & (\mathbf{x}_h^+)^\top \mathbf{1} = D_h \left(1 - \boldsymbol{\phi}_h^\top \mathbf{w}_h + \xi_{hs}\right), & \text{for } h \in \mathcal{H}(m) \\ & (\mathbf{x}_i^+)^\top \mathbf{1} = (\mathbf{x}_i^-)^\top \mathbf{1}, & \text{for } i \in \mathcal{H}_I \\ & (\mathbf{x}_i^-)^\top \mathbf{1} \leq \hat{s}_i + u_i, & \text{for } i \in \hat{\mathcal{H}} \\ & x_a = \gamma_a(\theta_{i(a)} - \theta_{j(a)}), & \text{for } a \in \mathcal{A}^E \\ & x_a \leq \gamma_a(\theta_{i(a)} - \theta_{j(a)}) + M(1 - z_a), & \text{for } a \in \mathcal{A}^N \\ & x_a \geq \gamma_a(\theta_{i(a)} - \theta_{j(a)}) - M(1 - z_a), & \text{for } a \in \mathcal{A}^N \\ & (\pi/4) \geq \theta_{i(a)} - \theta_{j(a)} \geq -(\pi/4), & \text{for } a \in \mathcal{A}^E \\ & (\pi/4)z_a \geq \theta_{i(a)} - \theta_{j(a)} \geq -(\pi/4)z_a, & \text{for } a \in \mathcal{A}^N \end{cases} \tag{12}$$

Note that $\hat{Q}_\xi(\boldsymbol{\lambda}; [C_g\ 0], [1\ 1])$ is piecewise constant with respect to $\mathbf{w}$ withing the set of $\boldsymbol{\lambda}$ for which there exist a feasible power flow in (12). We have the following relation:

$$\hat{G}(\mathbf{C}, \boldsymbol{\rho}) \ \leq \ \hat{G}([C_g\ 0], [1\ 1])$$

While the computation of $\hat{G}([C_g\ 0], [1\ 1])$ does not require the selection of $\mathcal{L}_a(x_a)$ around $\hat{x}_{a,1} \dots \hat{x}_{a,T}$ (as losses are equal to recoveries at zero cost), its optimal flow can be used as an initial guess for the actual flow in the resolution of (10) to select $\hat{x}_{a,0}$. Contextually, we define the resolution procedure below:

(i) Solve (12) to obtain $\hat{G}([C_g\ 0], [1\ 1])$ and an initial guess of the flow variables and the operator decisions, that we denote as $\mathbf{x}^{UB}$ and $\boldsymbol{\lambda}^{UB}$, respectively.

(ii) Using the solution in (i), build the sequence $\{x_a^{UB} + \tau t\}_{t=0}^{T}$, with $\tau = (\min\{s_{i(a)}, s_{j(a)}\} - x_a^{UB})/T$.

(iii) Using the linearization knots in (ii), compute $\hat{Q}_\xi(\boldsymbol{\lambda}^{UB}; \mathbf{C}, \boldsymbol{\rho})$, obtaining a lower bound $\hat{G}^{LB}$ to the profit.

(iv) Using $\hat{G}([C_g\ 0], [1\ 1])$ and $\hat{G}^{LB}$ to generate valid inequalities of the operator profit and the previously defined knots $\{x_a^{UB'} + \tau t\}_{t=0}^{T}$, solve the final two-stage stochastic problem (10).

As described in the next two sections, this solution approach is applied on a comprehensive power system data set from the Saudi Electricity Company, uncovering the value of the proposed integrated planning.

6 Integrated data on a centralized power system

The modeling design presented in section 3.2 has been tailored to fit the empirical setting presented in this section. We interact with SEC, a leading electricity company active in Saudi Arabia, obtaining a data set including $|\mathcal{H}| = 383$ stations that are divided into $|\mathcal{H}(1)| = 15$ genstats, $|\mathcal{H}(2)| = 44$ transmission stations (transtat), $|\mathcal{H}(3)| = 163$ distribution stations (diststat) and 1,156,648 active consumers grouped into $|\mathcal{H}(4)| = 163$ concent. These stations can be interconnected using $|\mathcal{A}| = 3480$ transmission linkages, where $|\mathcal{A}^E| = 402$ (working lines) and $|\mathcal{A}^N| = 34401$ (candidate new lines).

Most of the shares of the sole electrical utility responsible for the generation, transmission, distribution and pricing of the electricity are government owned. SEC manages the supply of electric power via four operating regions (which are ruled by separated entities within SEC) namely, Eastern, Western, Central and Southern. Focusing on the latter region, Table 1 provides a summary information about the main characteristics of each station.

		Genstat	Transtat	Diststat	Concent
Current capacity	Mean	1803.33	767.05	184.76	144.82
	Variance across nodes	1409809	106505	4112	2945
Maximum capacity	Mean	2147.20	1107.95	220.86	158.82
	Variance across nodes	2215280	129063	3698	3605
Observed electricity flow	Mean	-	39.21	3.55	0.89
	Variance across nodes	-	16476	606	146
number of units		15	44	163	163

Table 1: Mean and variance of the station capacities (in Megawatt) and observed power flow in SEC.

At the consumption level, the observed flows are averaged on an annual basis, consistently with time horizon of infrastructural changes in SEC. This simplification may circumvent the hourly fluctuations of the power demand, while allowing capturing a stable behavior for the purpose of price setting and capacity expansion. From Table 1, one can observe that the station capacities are underused. Moreover, the network connectivity is particularly low (i.e. only 1.2 % of the possibly feasible lines connecting substations are constructed).

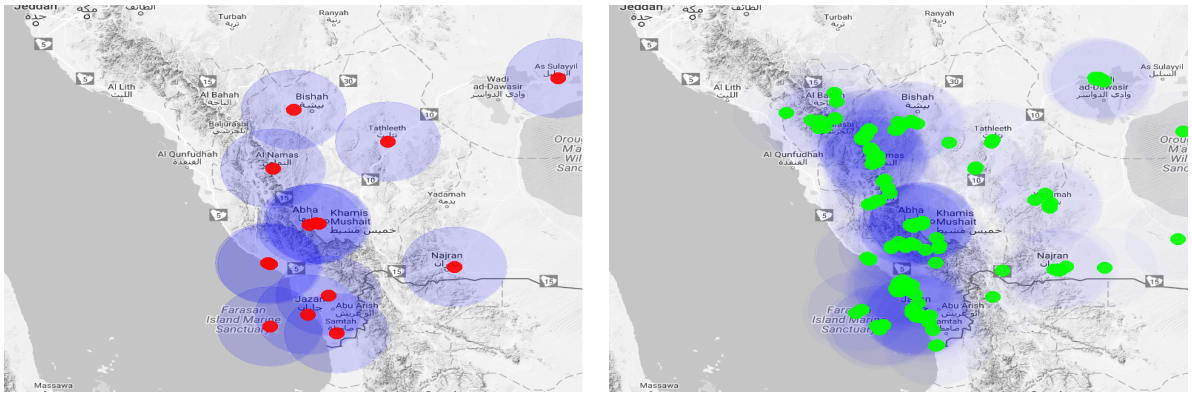

(a) Generation map in the Southern Region.

(b) Consumption map in the Southern Region.

Figure 1: Saudi generation and consumption areas

Fig. 1 shows the geographical distribution of the generation stations (left side) and the consumption centers (right side). On the figure, we can see that the power demand and its generation are not equally distributed throughout the Southern region of Saudi Arabia. This feature entails an additional layout difficulty for the electricity distribution and capacity expansion, where lines have different production costs and associated conductance and susceptance levels.

As described in Subsection 3.1, in most electricity markets prices vary for residential, commercial and industrial customers, and depend on the actual consumption level. Table 2 summarizes prices distribution among these categories.

Consumption level	Residential	Commercial	Agricultural	Governmental	Industrial
1 – 2000 Kwh	5	16	10	32	18
2001 – 4000 Kwh	10	16	10	32	18
4001 – 6000 Kwh	20	24	12	32	18
6001 – 8000 Kwh	30	24	12	32	18
> 8000 Kwh	30	30	16	32	18

Table 2: Power prices and levels for all categories of services (Council of Minister Decree n. 95 dated 28/01/2015).

In our model we consider a representative price level for each consumption center. Extensions to user types would entail enlarging the number of consumption centers by considering the cross combinations between locations and user types. In fact, the $1,156,648$ consumers are grouped in 163 locations, which have been aggregated in accordance with the consumer meters architecture. A graphical illustration of the dynamic consumption level in each of the 163 locations from in 2012 to 2016 is presented in Fig. 2.[16]

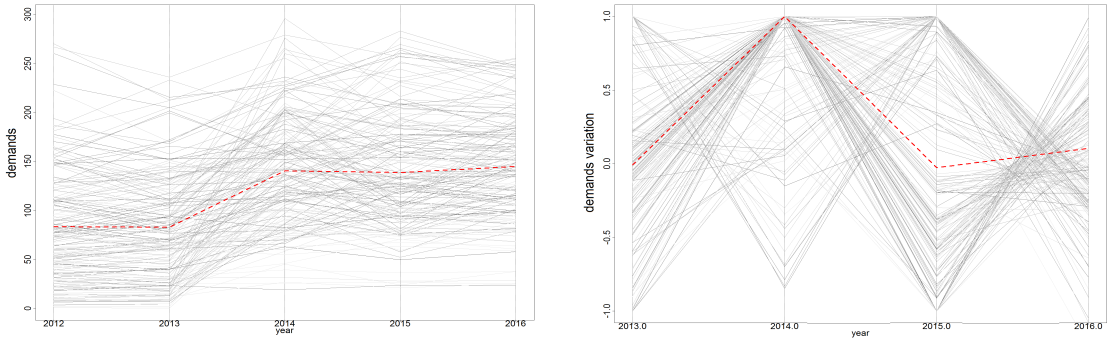

(a) Consumption levels.

(b) Relative consumption variations.

Figure 2: Consumption level (right panel) and relative consumption variation (left panel) in each of the 163 locations.

7 Computational tests and empirical analysis

As already discussed in sections 1 and 2, studies have shown theoretical and empirical evidence suggesting strong trade-offs between pricing and expansion in network management problems (Basar & Srikant 2002, Altman et al. 2006, López-Ramos et al. 2019). In line with these analysis, Section 4 explored the need and opportunity of capacity expansions and price variation in four stylized cases of centralized power systems.

[16] By fitting an auto-regressive model of order one with location effects and time trend, we observed an almost deterministic annual demand process with a coefficient of determination of 0.9495.

Using the power system data set described in the previous section and the linearized formulation (10), three types of analysis are conducted hereafter under different cost configurations and parameter settings to uncover the value of the proposed integrated planning:

- In Subsection 7.1, a profit sensitivity analysis is conducted to assess the impact of marginal costs and demand elasticity on the opportunity of price variation and capacity expansion, comparing the expected profit solution with the observed SEC profit. To emphasize the benefit of integrated decisions, the same analysis is replicated by fixing prices at the current level.

- In Subsection 7.2, the role of the demand uncertainty is studied in line with the analysis in Section 4 to relate the pricing and expansion decisions to the consumption knowledge and its indirect effect on profit.

- In Subsection 7.3, we go deeper into the computational aspects of the solving procedure to assess the goodness of the PWL approximation and the optimality bounds, as defined in Section 5.

The first two numerical tests involve a battery of $2^6 = 64$ problem instances created out of a 6–factor experiment fixed at two levels. In these tests, we consider three demand scenarios parameterized as $\hat{D}_h - SD\pi_d$, where π_d is a fluctuation from the expected demand and $SD = 33.14$ is the standard deviation estimated from the data set.[17] The six factors are listed below:

β: proportionality constant to the line distances, fixed at values $\{0.1, 0.5\}$;
C_r: proportionality constant to the recovery cost, fixed at values $\{0.0001, 0.0005\}$;
C_g: proportionality constant to the generation cost, fixed at values $\{0.00001, 0.00005\}$;
π: vector of scenario probabilities, fixed at values $\{(1-\pi_0)/2, \pi_0, (1-\pi_0)/2\}$, with $\pi_0 = \{0.175, 0.5\}$;
$\boldsymbol{\phi}$: vector of demand variations, fixed at values $\{0.05, 0.1\}$;
$\mathcal{S}$: demand scenarios, fixed at levels $\pi_d = \{0.05, 0.1\}$.

The rest of parameters are set as follows. The number of approximation lines for the power losses term is set to $|\mathcal{T}| = 12$ (consistently with the analysis in Subsection 7.3); a 10% price variation is proposed, i.e. $\mu^+ = \mu^- = 0.1$; the maximum number of lines has been set to $B = 50$ and the maximum price variation across location at $\Theta = 20$ Saudi Riyals (the equivalent of 4.84 Euros or 5.33 US Dollars).

All optimization procedures involved in the solving mechanism are performed using the IBM ILOG CPLEX 12.7 implementation of the branch-and-cut algorithm on a R5500 work-station with processor Intel(R) Xeon(R) CPU E5645 2.40 GHz, and 48 Gbytes of RAM, under a Windows Server 2012 operative system.

7.1 Optimal energy production and distribution within the existing grid

Tables 3 and 4 compares the expected profit given by (10) with SEC profit, for the two respective cases of network expansion only and network expansion with pricing (i.e. integrated planning).[18] Each cell is obtained by averaging out four instances made of two combinations of π and $\mathcal{S}$, as described above. The profits are decomposed into their expected and observed revenues and cost components. The columns contain, from left to right, the expected revenue, the expected recovery cost, the expected generation cost and the investment cost. The last two columns of each table contain the expected profit and the observed SEC profit. The six rows

[17] We also tested higher number of scenarios with no sensible changes in the operator decisions, as the flows are averaged at the annual basis. However, the use of higher number of scenarios increased substantially the running time.

[18] For confidentiality reasons this profit has been estimated without a direct access to the company balance sheet. Building on the available data on the power flow across each line, SEC profit has been computed by fixing price variations and capacity expansion at zero and plugging the observed power flow (x_a variables) into problem (10).

of each table list the different combinations of construction costs weight β and the ratio between recovery and generation costs C_r/C_g.

The figures in all tables show an homogeneous expected revenue within levels of ϕ for the MILP and SEC solutions, suggesting that demand sensitivity is the main driving factor of the revenue term. This constant revenue is driven by the fact that the optimal prices are common in all the instances. Conversely the cost structure strongly fluctuates across the cost parameters. When the demand sensitivity to prices is low (i.e. $\phi = 0.05$) the optimized solution increases SEC profit by 39%, in the worse case, and by 140%, in the best case. When average demand sensitivity to prices is high (i.e. $\phi = 0.1$), the optimized solution increases SEC profit by 24%, in the worse case, and by 497%, in the best case. As a result, the current price level, distribution structure and recovery pattern give rise to substantial losses, which could have been avoided by proper integrated decisions.

β	$\frac{C_r}{C_g}$	Exp. Revenue		Exp. Recovery cost		Exp. Generation cost		Invest. cost		Exp. Profit	
		(10)	SEC	(10)	SEC	(10)	SEC	(10)	SEC	(10)	SEC
	2	1511633	1511633	138154	201756	9976	10692	288	0	469245	341614
0.1	10	1511633	1511633	402798	591759	5989	6415	334	0	-56103	-434116
	50	1511633	1511633	682219	1004238	2284	2138	403	0	-611310	-1254798
	2	1511633	1511633	138230	201756	9977	10692	1095	0	468284	341614
0.5	10	1511633	1511633	412502	604813	5992	6415	1425	0	-76605	-460224
	50	1511633	1511633	683644	1004238	2278	2138	1800	0	-615549	-1254798

Table 3: Solution comparison between (10) and SEC company for the case of no price variation ($\phi^+ = \phi^- = 0$). Figures are expressed in Saudi Riyals.

ϕ	β	$\frac{C_r}{C_g}$	Exp. Revenue		Exp. Recovery cost		Exp. Generation cost		Invest. cost		Exp. Profit	
			(10)	SEC	(10)	SEC	(10)	SEC	(10)	SEC	(10)	SEC
		2	1511697	1511633	138736	218551	9472	10692	225	0	502659	308024
	0.1	10	1511697	1511633	404539	638623	5693	6415	300	0	-25242	-527845
		50	1511697	1511633	706324	1092745	2121	2138	370	0	-625311	-1431812
0.05		2	1511697	1511633	139449	218551	9471	10692	916	0	500544	308024
	0.5	10	1511697	1511633	416712	655651	5698	6415	1299	0	-50593	-561900
		50	1511697	1511633	691713	1092745	2117	2138	1531	0	-597245	-1431812
		2	1511760	1511633	98028	166132	8969	10692	168	0	543064	412861
	0.1	10	1511760	1511633	269761	489320	5383	6415	276	0	203077	-229239
		50	1511760	1511633	446216	817296	1956	2138	403	0	-146534	-880914
0.1		2	1511760	1511633	97859	166132	8969	10692	790	0	542780	412861
	0.5	10	1511760	1511633	273781	497060	5386	6415	1098	0	194212	-244718
		50	1511760	1511633	446089	817296	1958	2138	1568	0	-147446	-880914

Table 4: Solution comparison between our MILP(10) and SEC company for the case of no pricing ($\phi^+ = \phi^- = 0$), low elastic demands ($\phi^+ = \phi^- = 0.05$) and high elastic demands ($\phi^+ = \phi^- = 0.1$). Figures are expressed in Saudi Riyals

Comparing tables 3 and 4, we observe an increase in profit of approximately 10% in all the analysed instances, when pricing decisions are included along with the network expansion.

To emphasize the interdependency of operator decisions on power losses and recovery, tables 5 and 6 shows the divergences occurring congestion-like type of costs are ignored. The first four columns report the differences in the expected profit and expansion when looses are not considered (columns 3-6), while subsequent four columns report differences when losses are not recovered (columns 7-10).

β	$\frac{C_r}{C_g}$	Without losses				Without recovery			
		Abs GAP	Rel GAP	Δz	Δu	Abs GAP	Rel GAP	Δz	Δu
0.1	2	-1032447	- 220 %	-28	0	755347	161 %	19606	247
	10	-1561772	- 2784 %	-33	0	755873	1347 %	24983	8387
	50	-2120955	- 347 %	-40	0	756428	124 %	33022	16754
0.5	2	-1033408	- 221 %	-21	0	52569	11 %	11636	175
	10	-1582273	- 2066 %	-29	0	404402	528 %	15307	885
	50	-2125193	- 345 %	-40	0	756432	123 %	19138	1254

Table 5: Impacts of power losses and their recovery on the solution of the MILP(10) for the case of no price variation ($\phi^+ = \phi^- = 0$). Figures are expressed in millions of Saudi Riyals

ϕ	β	$\frac{C_r}{C_g}$	Without losses				Without recovery			
			Abs GAP	Rel GAP	Δz	Δu	Abs GAP	Rel GAP	Δz	Δu
0.05	0.1	2	-999593	- 199 %	-24	0	721366	144 %	19493	168
		10	-1531273	- 6066 %	-32	0	721894	2860 %	24445	9338
		50	-2135119	- 341 %	-35	0	722494	116 %	33776	18053
	0.5	2	-1001709	- 200 %	-21	0	675087	135 %	19045	100
		10	-1556623	- 3077 %	-30	0	406309	803 %	15267	282
		50	-2107053	- 353 %	-36	0	722466	121 %	19508	653
0.1	0.1	2	-959188	- 177 %	-18	0	753352	139 %	14358	278
		10	-1302953	- 642 %	-28	0	757535	373 %	20646	2958
		50	-1656342	- 1130 %	-40	0	763649	521 %	28249	5407
	0.5	2	-959472	- 177 %	-17	0	668885	123 %	18251	131
		10	-1311818	- 675 %	-26	0	399932	206 %	12200	199
		50	-1657254	- 1124 %	-40	0	763650	518 %	13879	788

Table 6: Impacts of power losses and their recovery on the solution of the MILP(10) for the case of no pricing ($\phi^+ = \phi^- = 0$), low elastic demands ($\phi^+ = \phi^- = 0.05$) and high elastic demands ($\phi^+ = \phi^- = 0.1$). Figures are expressed in millions of Saudi Riyals

The results of tables 3 and 4 show significant differences in both situations for low and high elastic demands. When losses are not considered, less lines are constructed (i.e., Δz values are negative), while the opposite happens when losses are considered without recovery. Next, comparing tables 3 and 4, we observe that neglecting price variations when the power network is expanded induces a larger expansion level in all the analyzed instances.

To cast a closer look into the leading effects behind these discrepancies, Table 7 reports elasticities of the tested parameters (assuming linear relationships with order-two interaction factors) with respect to the SEC profit, the expected profit under the integrated planning and their gap.

The main impact on the profit values hinges on the ratio between the recovery and the generation costs. This supports the aforementioned indirect spillover of prices and expansion to the scaling costs induced by power losses. In fact, as discussed in Section 1, when the recovery cost is much larger than the generation cost, pricing and expansion can act as substitutes. In fact, while prices have a direct impact on the total company revenue, they affect indirectly the scaling distribution costs, through their relations with power demands. This indirect effect acts on the company cost structure by causing variations on the power flow at each transmission line, similar to the outcome of building (or dismantling) parallel lines. Clearly, which of these substitutable strategies are the most profitable depends on the infrastructure costs weight β and demand elasticity ϕ.

Factor	Exp. profit		
	SEC	MILP(10)	Gap
$\frac{c_r}{c_g}$	-0.606	-0.585	0.062
β	-0.008	-0.006	0.009
π_0	0.017	0.031	0.004
π_d	-0.009	-0.031	-0.027
ϕ	0.199	0.291	-0.049
$\frac{c_r}{c_g} : \beta$	0.003	0.010	0.007
$\frac{c_r}{c_g} : \pi_0$	0.018	0.024	-0.008
$\frac{c_r}{c_g} : \pi_d$	0.004	-0.010	-0.024
$\frac{c_r}{c_g} : \phi$	0.093	0.142	-0.013
$\beta : \pi_0$	0.008	0.005	-0.013
$\beta : \pi_d$	0.008	0.011	-0.002
$\beta : \phi$	0.003	0.001	-0.006
$\pi_0 : \pi_d$	0.009	-0.010	-0.037
$\pi_0 : \phi$	0.006	0.010	0.001
$\pi_d : \phi$	0.002	-0.010	-0.020

Table 7: Elasticities of the tested parameters with respect to the SEC profit (left column), the MILP(10) profit (center column) and their gap (right column). The coefficients are estimated using ordinary least square on standardized data.

7.2 Cost sensitivity of line creation and station expansion

This subsection digs into the effect of the demand uncertainty on prices and expansion, to empirically support the theoretical results studied in Section 4. As a matter of fact, while our focus on average demands over the annual period allows for an almost deterministic characterization at each location level, the effect of any departure of this deterministic characterization should be computationally assessed. To do so, we rely on the 6–factor experiment presented at the beginning of this section, where three scenarios are considered: an average scenario (which coincides with the expected demands) and two tail scenarios (giving rise to departures from this central point). These scenarios are parameterized as $\hat{D}_h - SD\pi_d$, where the average scenario occurs with probability π_0 and the two tail scenarios with probability $(1-\pi_0)/2$.

		Subnetwork	$\pi_d = 0.01$		$\pi_d = 0.1$	
		π_0	0.175	0.5	0.175	0.5
$\phi = 0.05$	Built Lines	Gen-Tran	0.00	0.00	0.00	0.00
		Tran-Dist	10.63	6.50	10.50	13.38
		Dist-Concent	19.25	19.63	19.88	19.88
	Built Cost	Gen-Tran	0.00	0.00	0.00	0.00
		Tran-Dist	203.34	132.30	194.40	225.67
		Dist-Concent	558.80	598.58	588.37	618.40
	Price variation	Destinations	7.83	7.83	7.83	7.83
$\phi = 0.1$	Built Lines	Gen-Tran	0.00	0.00	0.13	0.00
		Tran-Dist	9.88	8.75	10.00	9.13
		Dist-Concent	17.63	19.38	18.38	18.88
	Built Cost	Gen-Tran	0.00	0.00	3.64	0.00
		Tran-Dist	206.60	153.32	199.34	164.45
		Dist-Concent	519.56	552.53	531.52	507.74
	Price variation	Destinations	7.83	7.83	7.83	7.83

Table 8: Summary on Line construction and price decisions depending on demand variation and scenario probabilities

Table 8 shows the effect of the values and probabilities of tail scenarios (capturing the departure from a deterministic case) on the optimal prices and expansion (given by solving (10)). As in the previous subsection, the results are reported for each level of ϕ, β and C_r/C_g. The rows provide, from up to down, the total number of constructed lines and its construction costs for each layer connecting consecutive stations. The last row indicates the average price variation for the consumption centers (destinations).

Independently of the degree of uncertainty, prices are optimally increased by 10%, while small variations are observed in the expansion pattern. Without regard to the degree of uncertainty, the optimized decisions tend to construct and invest more in new lines at the second and third subnetworks (i.e., between the transmission stations and the distribution stations, and between the latter and the consumption centers), due to the longer distances (and corresponding losses) in these subnetworks.

7.3 Computational performance

Table 9 shows the efficiency and correctness of the resolution procedure described in Section 5. The tables include (from left to right) the optimized profit and computing times for the upper and lower bounds (UB and LB, respectively), as well as the complete MILP incorporating the two bounds as valid inequalities. Additionally, the middle column indicates the relative gap in percentage between these bounds. The 9 rows of each table list the different combinations of β and C_r/C_g.

ϕ	β	$\frac{C_r}{C_g}$	Profits in millions of Saudi Riyals			GAP	CPU times in seconds		
			UB	LB	MILP(10)		UB	LB	MILP(10)
0.05	0.1	2	780384	357942	502659	54%	29	188	1728
		10	784162	-452728	-25242	158%	32	171	4299
		50	787939	-1325323	-625311	268%	30	230	7200
	0.5	2	780384	357942	500544	54%	29	192	885
		10	784162	-483237	-50593	162%	32	212	4112
		50	787939	-1325323	-597245	268%	30	234	7200
0.1	0.1	2	752440	443555	543064	41%	33	192	3301
		10	756814	-130492	203077	117%	35	155	4138
		50	761188	-724108	-146534	195%	38	231	7200
	0.5	2	752440	443555	542780	41%	31	183	568
		10	756814	-143527	194212	119%	31	169	4142
		50	761188	-724108	-147446	195%	32	190	7200

Table 9: Performance results averaged on probability combinations for the case of low elastic demands $\phi^+ = \phi^- = 0.05$ and high elastic demands $\phi^+ = \phi^- = 0.1$.

In all the 64 analyzed instances, the solver returned a feasible solution within a low mipgap. In four cases, corresponding to the parameter configuration $C_r/C_g = 50$, the CPLEX solver stopped having reached the time limit (7200 seconds). However even in those cases, the mipgap was below 0.1 and the computing times of the bounds remain always low (i.e., between one and two orders of magnitude compared to the computing times of the complete MILP). It is worth mentioning that some tests were carried out solving (10) without the bounds, resulting in a poor performance. Just in a few cases, the resolution with a MIPGAP of 0.1 has been achieved within the time limit, when bounds have not been included.

To complete the analysis of the computational performance, we cast a closer look into accuracy of the PWL approximation (7) for different values of $\mathcal{T}$. On the left panel of Fig. 3, the evolution of the running time (in seconds) is depicted, while the right panel illustrates the evolution of the expected profit in millions of Saudi

Riyals. Both plots are built averaging out 8 instances (at each of the 5 depicted points), obtained by the cross-combinations of C_r, C_g and β at two levels and reporting the traces of the mean + standard deviation/2 (gray line), mean (blue line) and mean - standard deviation/2 (orange line). For this stylized test, we assume a unique scenario for the electricity demand (deterministic case) fixed at its expected level and no price variation.

On the one hand, we observe that the profit value stabilizes at $|\mathcal{T}| > 3$. On the other hand, only a tiny increase in running time is observed when $|\mathcal{T}| > 3$, being below of 2 hours.[19]

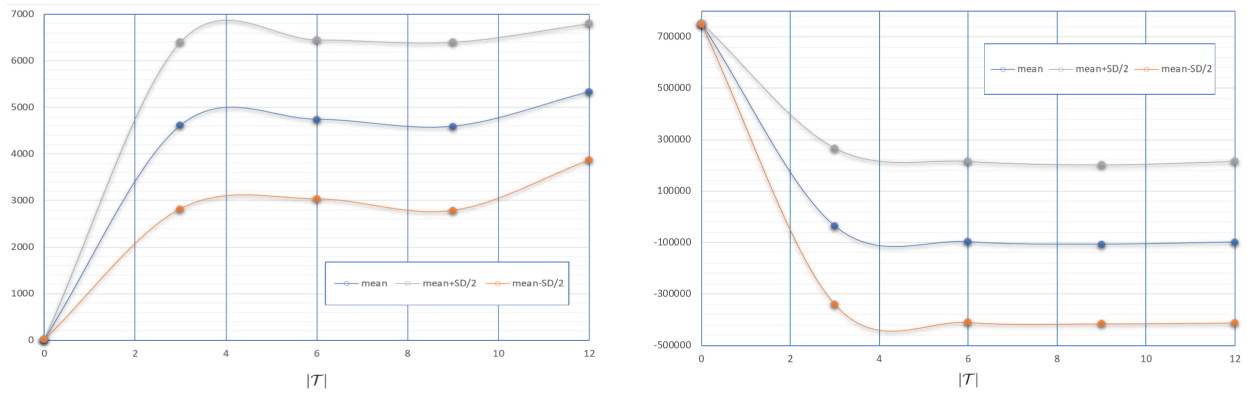

(a) Running time.

(b) Objective function.

Figure 3: Average performance as a function of $|\mathcal{T}|$, where the 5 points correspond to $|\mathcal{T}| = 0, 3, 6, 9, 12$. Panel (a) reports the running time (in seconds), while panel (b) reports the profit (in millions of Saudi Riyals).

Overall, the proposed linearization procedure described in subsection 3.3 provides a good estimation of the power losses, needing a low number of PWL terms for approaching the quadratic constraints associated with the power flows.

8 Conclusions and further research

This work presents an integrated planning model for power pricing and network expansion, endogenizing the scaling costs from power losses. Aiming at uncovering the value of integrated decisions, the modeling contribution of this work pivots on the relationship between electricity pricing and network expansion, which is magnified by the scaling costs from power losses. In fact, while the substitutability pattern between pricing and expansion has been largely overlooked in the power flow optimization literature, this becomes particularly relevant in centralized electricity markets (where the headquarters are enabled to take decisions over a wide range of operational factors).

We provide a computationally treatable resolution mechanism, where the non-linear terms in the model are linearized based on regularity conditions of the power flow (as described in Subsection 3.3). Allowing for stochastic demands, the two-stage stochastic program is then approximated by a mixed-integer linear programming problem, using a standard multi-scenario formulation. Upper and lower bounds to the resulting model are computed in a manner that allows the generation of PWL pivots for the linearization of the losses function (as described in Section 5).

A case study representing the actual integrated power flow network of the Southern Region of Saudi Arabia is proposed. Currently, the Saudi Electricity Company manages a network containing 383 stations and 402

[19] It is worth saying that the values of mean, mean + standard deviation/2 and mean - standard deviation/2 for the objective function and computational time are rather similar for $|\mathcal{T}| = 0$.

transmission lines. However, the station capacities are only working at their 46 % on average, and the network connectivity is significantly low (only 1.2 % of the possible feasible lines are constructed). Our methodology allows SEC to optimally evaluate the balance between recovery and generation, as well as the one between pricing and expansion. The results on a battery of 64 problem instances show improvements on the expected company profit between 39% -140% for low demand sensitivity, and between 24% -497% for high demand sensitivity, when taking integrated decisions. Next to it, we explored the differences in the optimal expansion when looses are not considered and when losses are not recovered. The results reveal substantial expansion variations, induced by the lack of integration, as well as an underestimation/overestimation of the expected profit.

In conclusion, the proposed integrated approach for centralized power systems allows dealing with a class of operational research problems that has been overlooked or only partially addressed in the recent literature. Our modeling framework can be extended to cope with further features arising in other economic and national contexts, such as: 1) storage systems for renewable energies (Olave-Rojas et al. 2017, Lara et al. 2018), 2) multi-period decisions on network expansion (Lara et al. 2018), 3) designing a resilient networks to failures and destruction (Benavides et al. 2013, Wang et al. 2016), 4) integration of microgrids (Ackooij et al. 2018), 5) decentralized electricity markets (Le Cadre et al. 2015, Lohmann & Rebennack 2016). When incorporating some of these features several algorithmic enhancements should be considered (i.e., specialized decomposition approaches (Castro et al. 2017, Lohmann & Rebennack 2016, Steeger & Rebennack 2017, Lara et al. 2018), bi-level reformulations (Ackooij et al. 2018)), resulting in a potential stream of future research.

References

Ackooij, W., de Boeck, J., Detienne, B., Pan, S., & M, P. (2018). Optimizing power generation in the presence of micro-grids. *European Journal of Operational Research*, *271*, 450–461.

Ahuja, R. K., Magnanti, T. L., & Orlin, J. B. (1993). *Network Flows*. Englewood Cliffs, NJ: Prentice-Hall.

Al-Gwaiz, M., Chao, X., & Wu, O. Q. (2016). Understanding how generation flexibility and renewable energy affect power market competition. *Manufacturing & Service Operations Management*, *19*, 114–131.

Alguacil, N., Motto, A. L., & Conejo, A. J. (2003). Transmission expansion planning: A mixed-integer lp approach. *IEEE Transactions on Power Systems*, *18*, 1070–1077.

Altman, E., Boulogne, T., El-Azouzi, R., Jimnez, T., & Wynter, L. (2006). A survey on networking games in telecommunications. *Computers & Operations Research*, *33*, 286–311.

Atamtürk, A., & Zhang, M. (2007). Two-stage robust network flow and design under demand uncertainty. *Operations Research*, *55*, 662–673.

Aussel, D., Brotcorne, L., Lepaul, S., & von Niederhäusern, L. (2019). A trilevel model for best response in energy demand-side management. *European Journal of Operational Research*, .

Basar, T., & Srikant, R. (2002). Revenue-maximizing pricing and capacity expansion in a many-users regime. In *Proceedings.Twenty-First Annual Joint Conference of the IEEE Computer and Communications Societies* (pp. 294–301 vol.1). volume 1.

Benavides, A., Ritt, M., Buriol, L., & Fransa, P. (2013). An iterated sample construction with path relinking method: Application to switch allocation in electrical distribution networks. *Computers & Operations Research*, *40*, 24–32.

Birge, J. R., & Louveaux, F. (2011). *Introduction to stochastic programming*. Springer Science & Business Media.

Carpentier, J. (1979). Optimal power flows. *International Journal of Electrical Power & Energy Systems*, *1*, 3–15.

Castro, J., Nasini, S., & Saldanha-da Gama, F. (2017). A cutting-plane approach for large-scale capacitated multi-period facility location using a specialized interior-point method. *Mathematical programming*, *163*, 411–444.

Correa-Florez, C., Bolaños-Ocampo, R., & Escobar-Zuluaga, A. (2014). Multi-objective transmission expansion planning considering multiple generation scenarios. *Electrical Power and Energy Systems*, *62*, 398–409.

Dommel, H. W., & Tinney, W. F. (1968). Optimal power flow solutions. *IEEE Transactions on power apparatus and systems*, (pp. 1866–1876).

Fischetti, M., & Pisinger, D. (2018). Optimizing wind farm cable routing considering power losses. *European Journal of Operational Research*, *270*, 917–930.

Frank, S., & Rebennack, S. (2016). An introduction to optimal power flow: Theory, formulation, and examples. *IIE Transactions*, *48*, 1172–1197.

Frank, S., Steponavice, I., & Rebennack, S. (2012a). Optimal power flow: a bibliographic survey i. *Energy Systems*, *3*, 221–258.

Frank, S., Steponavice, I., & Rebennack, S. (2012b). Optimal power flow: a bibliographic survey ii. *Energy Systems*, *3*, 259–289.

Frank, S. M., & Rebennack, S. (2015). Optimal design of mixed acdc distribution systems for commercial buildings: A nonconvex generalized benders decomposition approach. *European Journal of Operational Research*, *242*, 710–729.

Fügenschuh, A., Geißler, B., & Gollmer, R. (2014). Mathematical optimization for challenging network planning problems in unbundled liberalized gas markets. *Energy Systems*, *5*, 449–473.

Garver, L. L. (1970). Transmission network estimation using linear programming. *IEEE Transactions on power apparatus and systems*, *89*, 1688–1697.

IRENA (2019). *Renewable Energy Market Analysis: GCC 2019*. International Renewable Energy Agency.

Jenabi, M., Fatemi-Ghomi, S., Torabi, S., & Hosseinian, S. (2015). Acceleration strategies of benders decomposition for the security constraints power system expansion planning. *Annals of Operational Research*, *235*, 337–369.

Jensen, P. A., & Bhaumik, G. (1977). A flow augmentation approach to the network with gains minimum cost flow problem. *Management Science*, *23*, 631–643.

Kök, A. G., Shang, K., & Yücel, Ş. (2016). Impact of electricity pricing policies on renewable energy investments and carbon emissions. *Management Science*, *64*, 131–148.

Kovacevic, R. M. (2019). Valuation and pricing of electricity delivery contracts: the producers view. *Annals of Operations Research*, *275*, 421–460.

Krasko, V., & Rebennack, S. (2017). Chapter 15: Global optimization: Optimal power flow problem. In *Advances and Trends in Optimization with Engineering Applications* chapter 15. (pp. 187–205).

Lahdelma, R., & Hakonen, H. (2003). An efficient linear programming algorithm for combined heat and power production. *European Journal of Operational Research*, *148*, 141–151.

Lara, C., Mallapragada, D., Papageorgiou, D., Venkatesh, A., & Grossmann, I. (2018). Deterministic electric power infraestructure planning: Mixed-integer programming model and nested decomposition algorithm. *European Journal of Operational Research*, *271*, 1037–1054.

Le Cadre, H., Papavasiliou, A., & Smeers, Y. (2015). Wind farm portfolio optimization under network capacity constraints. *European Journal of Operational Research*, *247*, 560–574.

Lium, A.-G., Crainic, T. G., & Wallace, S. W. (2009). A study of demand stochasticity in service network design. *Transportation Science*, *43*, 144–157.

Lohmann, T., & Rebennack, S. (2016). Tailored benders decomposition for a long-term power expansion model with short-term demand response. *Management Science*, *63*, 1657–2048.

López-Ramos, F., Nasini, S., & Guarnaschelli, A. (2019). Road network pricing and design for ordinary and hazmat vehicles: Integrated model and specialized local search. *Computers & Operations Research*, *109*, 170–187.

Olave-Rojas, D., Alvarez-Miranda, E., Rodriguez, A., & Tenreiro, C. (2017). An optimization framework for investment evaluation of complex renewable energy systems. *Energies*, *10*, 1–26.

Özdemir, O., Muñoz, F., Ho, J., & Hobbs, B. F. (2016). Economic analysis of transmission expansion planning with price-responsive demand and quadratic losses by successive lp. *IEEE Transactions on Power Systems*, *31*, 1096–1107.

Papier, F. (2016). Managing electricity peak loads in make-to-stock manufacturing lines. *Production and Operations Management*, *25*, 1709–1726.

Rajarman, R., Alvarado, F., Maniaci, A., Camfield, R., & Jalali, S. (1998). Determination of location and amount of series compensation to increase power transfer capability. *IEEE Transactions on Power Systems*, *13*, 294–300.

Rebennack, S., & Kallrath, J. (2015). Continuous piecewise linear delta-approximations for univariate functions: Computing minimal breakpoint systems. *Journal of Optimization Theory and Applications*, *167*, 617–643.

Rebennack, S., & Krasko, V. (2019). Piecewise linear function fitting via mixed-integer linear programming. *INFORMS Journal on Computing*, .

Roh, J. H., Shahidehpour, M., & Fu, Y. (2007). Market-based coordination of transmission and generation capacity planning. *IEEE Transactions on Power Systems*, *22*, 1406–1419.

Romero, R., Montincelli, A., Garcia, A., & Haffner, S. (2002). Test systems and mathematical models for transmission network expansion planning. *IEE Proceedings - Generation, Transmission and Distribution*, *149*, 27–36.

Shen, X., Liu, Y., & Liu, Y. (2018). A multistage solution approach for dynamic reactive power optimization based on interval uncertainty. *Mathematical Problems in Engineering*, *2018*, 1–10.

Steeger, G., & Rebennack, S. (2017). Dynamic convexification within nested benders decomposition using lagrangian relaxation: An application to the strategic bidding problem. *European Journal of Operational Research*, *257*, 669–686.

Vielma, J. P., & Nemhauser, G. L. (2011). Modeling disjunctive constraints with a logarithmic number of binary variables and constraints. *Mathematical Programming*, *128*, 49–72.

Waller, S. T., & Ziliaskopoulos, A. K. (2001). Stochastic dynamic network design problem. *Transportation Research Record*, *1771*, 106–113.

Wang, Q., McCalley, J., Zheng, T., & Litvinov, E. (2016). Solving corrective risk-based security-constrained optimal power flow with lagrangian relaxation and benders decomposition. *Electrical Power and Energy Systems*, *75*, 255–264.

Zhou, Y., Scheller-Wolf, A., Secomandi, N., & Smith, S. (2019). Managing wind-based electricity generation in the presence of storage and transmission capacity. *Production and Operations Management*, *28*, 970–989.

Zou, J., Ahmed, S., & Sun, X. A. (2019). Multistage stochastic unit commitment using stochastic dual dynamic integer programming. *IEEE Transactions on Power Systems*, *34*, 1814–1823.